DELFT UNIVERSITY OF TECHNOLOGY

DEPARTMENT OF AEROSPACE ENGINEERING

Report VTH - 213

THE CALCULATION OF THE R.M.S. VALUE OF AN AIRCRAFT'S NORMAL ACCELERATION DUE TO GAUSSIAN RANDOM ATMOSPHERIC TURBULENCE

by

J.C. van der Vaart

DELFT - THE NETHERLANDS

March 1976

DELFT UNIVERSITY OF TECHNOLOGY

DEPARTMENT OF AEROSPACE ENGINEERING

Report VTH-213

THE CALCULATION OF THE R.M.S. VALUE OF AN AIRCRAFT'S NORMAL ACCELERATION DUE TO GAUSSIAN RANDOM ATMOSPHERIC TURBULENCE

by

J.C. van der Vaart

DELFT - THE NETHERLANDS

March 1976

SUMMARY

It is shown in this Report that a theoretical calculation of the variance, or the r.m.s. value of an aircraft's normal acceleration due to atmospheric turbulence characterized by the Dryden or von Karman power spectral densities is not possible if the time delay, characterizing the gust penetration effect, is approximated by the linear time-derivative description enabling the use of the gust derivatives $C_{Z_{\dot{\alpha}_g}}$, $C_{m_{\dot{\alpha}_g}}$ etc. (truncated Taylor series approximation of the turbulent field).

Such a calculation is shown to be possible if a first order Padé approximation is used to describe the penetration effect. The results thus obtained for an example aircraft are in very good agreement with those obtained by a pure time delay description.
In the case of other motion variables, where the linear time derivative approximation is theoretically possible, the results of the Padé approximation are also in better agreement with those obtained by a pure time delay.

Neglecting the penetration effect (point approximation of the aircraft in the turbulent field) is shown to cause gross errors, especially in the variance of the normal acceleration at points some distance away from the aircraft's c.g., a quantity affecting passenger and crew comfort.

Monte Carlo simulations using analogue computers and incorporating the time-derivative approximation of the gust penetration effect are shown to yield values of the variance of the normal acceleration that may be grossly in error depending, in a rather unexpected way, on the bandwidth of the electronic white noise generators used.

CONTENTS

LIST OF SYMBOLS

[A] system matrix

a_z aircraft's normal acceleration

b wing span

[B] forcing matrix

$\bar{c}$ aerodynamic mean chord

c.g. aircraft's centre of gravity

C_m pitching moment coefficient

$C_{m_q} = \dfrac{\partial C_m}{\partial \frac{q\bar{c}}{V}}$

$C_{m_u} = \dfrac{1}{\frac{1}{2}\rho V^2 S\bar{c}} \cdot \dfrac{\partial M}{\partial \hat{u}}$

$C_{m_\alpha} = \dfrac{\partial C_m}{\partial \alpha}$

$C_{m_{\alpha_g}} = \dfrac{\partial C_m}{\partial \alpha_g}$

$C_{m_{\dot{\alpha}}} = \dfrac{\partial C_m}{\partial \frac{\dot{\alpha}\bar{c}}{V}}$

$C_{m_{\dot{\alpha}_g}} = \dfrac{\partial C_m}{\partial \frac{\dot{\alpha}_g \bar{c}}{V}}$

C_X coefficient of aerodynamic force along the aircraft's X-axis

$C_{X_u} = \frac{1}{\frac{1}{2}\rho V^2 S} \cdot \frac{\partial X}{\partial \hat{u}}$

C_{X_o} = C_X in the steady flight condition

$C_{X_\alpha} = \frac{\partial C_X}{\partial \alpha}$

$C_{X_{\alpha_g}} = \frac{\partial C_X}{\partial \alpha_g}$

$C_{X_{\dot{\alpha}_g}} = \frac{\partial C_X}{\partial \frac{\dot{\alpha}_g \bar{c}}{V}}$

C_Z coefficient of aerodynamic force along the aircraft's Z-axis

$C_{Z_q} = \frac{\partial C_Z}{\partial \frac{q\bar{c}}{V}}$

$C_{Z_u} = \frac{1}{\frac{1}{2}\rho V^2 S} \cdot \frac{\partial Z}{\partial \hat{u}}$

C_{Z_o} = C_Z in the steady flight condition

$C_{Z_\alpha} = \frac{\partial C_Z}{\partial \alpha}$

$C_{Z_{\alpha_g}} = \frac{\partial C_Z}{\partial \alpha_g}$

$C_{Z_{\dot{\alpha}}} = - \frac{\partial C_Z}{\partial \frac{\dot{\alpha}\bar{c}}{V}}$

$C_{Z_{\dot{\alpha}_g}} = \frac{\partial C_Z}{\partial \frac{\dot{\alpha}_g \bar{c}}{V}}$

D_c $= \frac{\bar{c}}{V} \cdot \frac{d}{dt}$, dimensionless differential operator

I_y aircraft moment of inertia about the Y-axis

$[I]$ unit matrix

g acceleration due to gravity

h altitude

$H(\omega)$ transfer function

j $= \sqrt{-1}$

K_Y dimensionless radius of gyration, related to I_y by

$$\mu_c \cdot K_Y^2 = \frac{I_y}{\rho S \bar{c}^3}$$

l_h horizontal tail arm

L_g integral scale of turbulence

m $= \frac{W}{g}$, aircraft mass

m_q
m_u
m_α
m_{α_g}
$m_{\dot{\alpha}_g}$

stability and gust derivatives in abbreviated notation, see Appendix 1

M aerodynamic moment about the aircraft's Y-axis

$n_{c.g.}$ $= \frac{a_z}{g}$ normal acceleration factor at the aircraft's c.g.

P complex (Laplace) variable

q pitching velocity about the aircraft's Y-axis

$Re\{\ \}$ real part of a complex variable or function

S wing area

S_h horizontal tail area

t time

u change in $\vec{V}$ along the aircraft's X-axis

$\hat{u}$ $= \frac{u}{V}$

$\vec{V}$ velocity of the aircraft's c.g. relative to the earth, assuming no steady wind velocity

w_g vertical gust velocity

W aircraft weight

x distance along the aircraft's X-axis to a certain datum point

$\bar{x}$ state vector, vector of motion variables

x_u, x_α, $x_{\dot{\alpha}_g}$, x_θ, x_q stability-and gust derivatives in abbreviated notation, see Appendix 1

X	aerodynamic force along the aircraft's X-axis
$\bar{y}_g$	forcing function vector
z_q, z_u, z_α, $z_{\dot{\alpha}}$, z_{α_g}, z_θ	stability- and gust derivatives in abbreviated notation, see Appendix 2
Z	aerodynamic force along the aircraft's Z-axis
α	angle of attack, dimensionless change of $\vec{V}$ along the aircraft's Z-axis
α_g	$= \frac{w_g}{V}$, gust angle of attack
γ	flight path angle, angle between $\vec{V}$ and the horizontal plane
ε	downwash angle
θ	angle of pitch
μ_c	$= \frac{m}{\rho S \bar{c}}$ relative aircraft mass
ρ	air density
σ_x^2	variance of x
$\sigma_{x_1 x_2}$	covariance of x_1 and x_2
τ	time constant
$\Phi(\omega)$	power spectral density function (power spectum)

ω angular frequency

Subscripts and superscripts

c.g. centre of gravity

g gust, atmospheric turbulence

h horizontal tail

u output

w wing

w_g, α_g vertical turbulence

* conjugate of a complex variable or function

^{T} transpose of a vector or matrix

$^{-1}$ inverted matrix

Frame of reference

All aerodynamic forces and moments and stability derivatives are defined relative to a frame of reference having its origin 0 at the aircraft's centre of gravity c.g. The X-axis lies in the plane of symmetry, parallel to the velocity vector $\vec{V}$ in the steady flight condition, and is taken positive in the forward direction. The Y-axis is perpendicular to the plane of symmetry and is taken positive to starboard. The Z-axis is perpendicular to the X-O-Y-plane and positive downwards.

1. INTRODUCTION

The problem of calculating the response of an aeroplane to atmospheric turbulence can, similar to a concept given in Ref. 1, be separated into several distinct elements.

1) The statistical description of the turbulent field (the input),
2) The calculation of the aerodynamic forces and moments acting on an aircraft due to the turbulent field in terms of transfer functions,
3) The calculation of the transfer functions relating the aircraft motion variables to the gust-induced forces and moments,
4) The combination of the transfer functions and the input to obtain the output.

This concept is diagramatically shown in Fig. 1. Under the assumption that atmospheric turbulence is a stationary gaussian stochastic process and that aircraft perturbations due to atmospheric turbulence can be described by linear differential equations, ensemble properties such as the variance or the r.m.s. value of motion variables can be calculated by a number of well established methods.
In practical calculations atmospheric turbulence is usually characterized by either of the wellknown power spectral densities (or power spectra) due to Dryden or von Karman (see Ref. 2). The transfer functions relating the aircraft's output to the gust forces and moments may, under the assumption of linearity, conveniently be obtained using linear system theory.

Restricting the discussion in this Report to symmetric aircraft motions due to vertical turbulence velocities only, a first assumption commonly made is that the gust velocities are uniformly distributed over the wing span.

In the majority of the publications on calculations of aircraft response to turbulence it appears that the aforementioned assumptions are, although sometimes tacitly, frequently made. See for instance Refs. 3, 4 and 18.

As to the aerodynamic transfer functions, relating forces and moments and the vertical gust velocity, a further assumption is often made i.e. that the growth of the lift and pitching moment of an aircraft wing due to a gust is instantaneous rather than occurring over a certain time as characterized by the so called Küssner function (see Ref. 5). If this effect is ignored, the pertaining aerodynamic transfer functions become identical with the derivatives $C_{Z_{w_\alpha}}$ and $C_{m_{w_\alpha}}$ of the wing.

An example where a Küssner function is explicitly used for modelling the lift growth, can be found in Ref. 3.

Another phenomenon leading to an aerodynamic transfer function is the so called "gust penetration effect". This effect can roughly be described as caused by different parts of the aircraft (especially the wing and the tail) being hit by the same gust at different instants in time.
By assuming the gust velocities to be uniformly distributed along the length of the aircraft as well as along the wing span, this effect is ignored and the "point approximation" of the aircraft in the turbulent field as discussed in Ref. 6 is obtained.

However, the gust penetration effect is shown in this Report to have a considerable influence on the normal acceleration. It can in principle very conveniently be modelled in a number of ways, as will be discussed in Chapter 3 of this Report. As a consequence it should be included in calculations of aircraft response to turbulence.

For aircraft of a conventional wing-tail lay-out with modest wing sweep, the gust penetration effect is usually considered to be mainly caused by the horizontal tail only, allowing the effect to be described by a pure time-delay characterized by the time interval $\tau = \frac{l_h}{V}$, l_h being the horizontal tail arm.

One way to describe the pure time-delay is by a linear time-derivative

approximation (Ref. 7), yielding the well known gust derivatives $C_{Z_{\dot{\alpha}_g}}$, $C_{m_{\dot{\alpha}_g}}$, etc., see for instance Ref. 8. The mathematical description thus obtained is similar to the one introduced by Etkin (Refs. 1 and 6). The turbulent gust field is then approximated locally by a Taylor series truncated after the linear terms, see also Chapter 3 of this Report.

When using this approximation some difficulties may be met when calculating the variance or the r.m.s. value of an aircraft's normal acceleration due to turbulence. It appears that if the Dryden (or von Karman) turbulence spectra are used, a calculation of the variance of the normal acceleration is in a strict sense not possible. This will be briefly explained in the second Chapter.

Chapter 3 deals in more detail with the gust penetration effect. The effect will be modelled in three ways i.e.:

1) by a pure time-delay,
2) by a first order Padé approximation of the pure time-delay,
3) by the first order time-derivative approximation (truncated Taylor series representation of the turbulent field).

The first two methods will be presented in such a way that the well-known gust derivatives $C_{Z_{\dot{\alpha}_g}}$ and $C_{m_{\dot{\alpha}_g}}$ of the third method may still be used, introducing only one new parameter, the tail arm l_h. It will be shown that the difficulty mentioned in calculating the normal acceleration r.m.s. can be circumvented by using either of the first two descriptions.

The power spectral densities and the variances of the normal acceleration at the centre of gravity and at other points along the aircraft's X-axis, thus calculated will be compared in Chapter 4 for an example aircraft assuming constant speed.

Further numerical examples are given in Chapter 5 for two more example aircraft.

2. THE AIRCRAFT'S NORMAL ACCELERATION DUE TO ATMOSPHERIC TURBULENCE

The aircraft's vertical velocity with respect to an inertial frame of reference is:

$$\dot{h} \approx V \gamma = V (\theta - \alpha)$$

The normal acceleration a_z at the centre of gravity (c.g.) is in horizontal flight and neglecting the influence of variations in V on a_z:

$$a_z = \ddot{h} = V \dot{\gamma} = V (\dot{\theta} - \dot{\alpha})$$

The normal acceleration factor $n_{c.g.} = \frac{\ddot{h}}{g}$ is then:

$$n_{c.g.} = \frac{V^2}{g\bar{c}} \left(\frac{\dot{\theta}\bar{c}}{V} - \frac{\dot{\alpha}\bar{c}}{V} \right) \qquad (1)$$

In Appendix 1 the differential equations governing the aircraft's motions due to vertical atmospheric turbulence are given. These are in the case of the first-order time derivative approximation of the penetration effec see Chapter 3 of this Report, in vector matrix notation:

$$\dot{\bar{x}} \cdot \frac{\bar{c}}{V} = [A] \cdot \bar{x} + [B] \cdot \bar{y}_g \qquad (2)$$

where $\bar{x}$ is the aircraft's state vector:

$$\bar{x} = \left(\hat{u} \quad \alpha \quad \theta \quad \frac{q\bar{c}}{V} \right)^T$$

and $\bar{y}_g$ the vector of the gust forcing functions, in this case:

$$\bar{y}_g = (\alpha_g \quad D_c\alpha_g)^T$$

The dimensionless time derivative $\frac{\dot{\alpha}\bar{c}}{V}$ is an element of $\dot{\bar{x}} \cdot \frac{\bar{c}}{V}$ in eq. (2) and thus a linear function of the motion variables (the elements of $\bar{x}$) and the forcing functions (input signals) α_g and $D_c\alpha_g$ (see Appendix 1):

$$\frac{\dot{\alpha}\bar{c}}{V} = z_u \cdot \hat{u} + z_\alpha \cdot \alpha + z_\theta \cdot \theta + z_q \cdot \frac{q\bar{c}}{V} + z_{\alpha_g} \cdot \alpha_g + z_{\dot{\alpha}_g} \cdot D_c\alpha_g \qquad (3)$$

In Ref. 9 it is demonstrated that due to the approximative description of the atmospheric turbulence by the Dryden spectrum (or, for that matter, by the von Karman spectrum) the use of these spectra yield an infinite value of the variance of $D_c\alpha_g$. According to eq. (3) the variance of $\frac{\dot{\alpha}\bar{c}}{V}$, and as a consequence of $n_{c.g.}$ (see eq. (1)), as well, will be infinite.
In this case only an approximate calculation of $\sigma^2_{n_{c.g.}}$ will be possible, setting $z_{\dot{\alpha}_g} = 0$, which is equivalent to setting $C_{Z_{\dot{\alpha}_g}} = 0$, see Appendix 1.

When studying passenger or crew comfort it is important to know the variance of n at arbitrary points in the aircraft as the level of normal accelerations along the aircraft's longitudinal axis may vary considerably, see for instance Refs. 3 and 4. Here a similar problem arises. Due to the effect of the angular acceleration $\dot{q}$, the normal acceleration factor n_x at a distance $x - x_{c.g.}$ aft of the centre of gravity is:

$$n_x = n_{c.g.} - \frac{\dot{q}}{g}(x - x_{c.g.}) = \frac{V^2}{g\bar{c}}\left(\frac{\dot{\theta}\bar{c}}{V} - \frac{\dot{\alpha}\bar{c}}{V} - \frac{x - x_{c.g.}}{\bar{c}} \cdot \frac{\dot{q}\bar{c}^2}{V^2}\right) \qquad (4)$$

Again $\frac{\dot{q}\bar{c}^2}{V^2}$ is an element of $\dot{\bar{x}} \cdot \frac{\bar{c}}{V}$ and thus a linear function of the elements of $\bar{x}$ and the forcing functions α_g and $D_c\alpha_g$:

$$\frac{\dot{q}\bar{c}^2}{V^2} = m_u \cdot \hat{u} + m_\alpha \cdot \alpha + m_\theta \cdot \theta + m_q \cdot \frac{q\bar{c}}{V} + m_{\alpha_g} \cdot \alpha_g + m_{\dot{\alpha}_g} \cdot D_c\alpha_g \qquad (5)$$

Comparing eqs. (5) and (4) it will be clear that $\sigma^2_{n_x}$ will also become infinite as $\sigma^2_{D_c\alpha_g}$ is infinite. Neglecting both z_{α_g} and m_{α_g} will, of course, result in a finite value of $\sigma^2_{n_x}$ but will, as will be shown in this Report, yield too gross an approximation of $\sigma^2_{n_x}$.

It is important to note that the variance of the normal acceleration will only become infinite in the case of theoretical calculations i.e. either by the integration of the power spectral density in the frequency-domain or by a time-domain method such as the one described in Ref. 10 (impulse response method).

In the case of a Monte Carlo analogue-simulation where turbulence signals are generated by filtering white noise, the computed variance of the normal acceleration will always be finite due to the limited bandwidth of electronic white noise generators. The result will, however be dependent on the bandwidth of the white noise generator used, as will be explained in Chapter 4.

As to the case of digitally computed time propagation of the variance of n, a similar phenomenon occurs, due to the effect of discretization; i.e. a limited bandwidth white noise signal is generated, see Ref. 11.

Since in real processes the value of the variance of $D_c\alpha_g$, i.e. the variance of the accelerations of the air particles in the turbulent atmosphere, cannot be infinite, a possible solution, mentioned in Ref. 12, would be to alter the power spectra and the corresponding auto-covariance functions of atmospheric turbulence such, that a finite value of $\sigma^2_{D_c\alpha_g}$ is obtained.

Rather than adapting the shape of the power spectra and choosing a finite numerical value of $\sigma^2_{D_c\alpha_g}$, the diffifulties can be circumvented by a number of different mathematical descriptions of the gust penetratio effect, still retaining the unaltered power spectra.

In the next Chapters it is shown that a calculation of the normal acceleration variance is possible either by describing the penetration effect by a pure time-delay or by a first order Padé approximation of the pure time delay. The first mathematical description allows a computation in the frequency-domain only, while the latter enables a computation in the frequency-domain as well as in the time-domain by methods as described in Refs. 10 and 11.

3. THE GUST PENETRATION EFFECT

3.1. Some remarks on lift and pitching moment growth

The growth of forces and moments due to entering - or penetrating - a discrete gust α_g bears some similarity with the time-delay effect caused by a change in angle of attack of the aircraft in still air.

The latter effect was first described by Cowley and Glauert and approximated by a pure time-delay $\tau = \frac{l_h}{V}$, Ref. 13. Jones and Fehlner (Ref. 14) theoretically showed this approximation to hold for aircraft motions below a certain frequency and moreover recognized that this concept could be extended to the effect of forces and moments caused by vertical gusts. The time lag appeared to be somewhat greater than indicated by the tail length l_h, thus accounting for the lift growth as characterized by the Küssner function mentioned in the introduction.

Although many rather more refined methods of calculating the lift and pitching moment growth of wings and wing-tail combinations have been introduced since (see Refs. 15, 16 and 17), either the lift or the pitching moment growth due to entering a gust, or both, are very often neglected in practical calculations. For example in Ref. 18 no lift or pitching moment growth is taken into account; in Ref. 3 a Küssner function is used to model the wing lift and pitching moment growth, but the penetration effect due to the horizontal tail is ignored. In Ref. 4, concerning the same aeroplane as Ref. 3, the penetration effect is modelled by a pure time-delay.

In Ref. 8 a concept similar to the one described by Etkin (Refs. 1 and 6), i.e. that of a Taylor series truncated after the linear terms, is used. Moreover it is shown in Ref. 8 that if the normal force and pitching moment due to vertical turbulence are described by:

$$C_{Z_g} = C_{Z_{\alpha_g}} \cdot \alpha_g + C_{Z_{\dot{\alpha}_g}} \cdot D_c \alpha_g$$

$$C_{m_g} = C_{m_{\alpha_g}} \cdot \alpha_g + C_{m_{\dot{\alpha}_g}} \cdot D_c\alpha_g$$

where $D_c\alpha_g$ is the dimensionless time-derivative $\dot{\alpha}_g \cdot \frac{\bar{c}}{V}$ of the gust angle of attack α_g, the gust derivatives $C_{Z_{\dot{\alpha}_g}}$ and $C_{m_{\dot{\alpha}_g}}$ are:

$$C_{Z_{\dot{\alpha}_g}} = C_{Z_{\dot{\alpha}}} - C_{Z_q} \tag{6}$$

$$C_{m_{\dot{\alpha}_g}} = C_{m_{\dot{\alpha}}} - C_{m_q} \tag{7}$$

The gust derivatives as defined by eqs. (6) and (7) are conveniently obtained if the stability derivatives with respect to $\dot{\alpha}$ and $\frac{q\bar{c}}{V}$ are known. They will be used in this Report.

In the following the gust penetration effect is assumed to be caused by the horizontal tail only and $C_{Z_{\dot{\alpha}_g}}$ and $C_{m_{\dot{\alpha}_g}}$ are considered to consist merely of contributions due to the tail.

Strictly speaking, the calculations and conclusions drawn in this Report are only valid for aircraft of a conventional wing-tail layout with modest wing-sweep. The effective time delay τ can, however, be considered as a lumped parameter, taking into account all lift and pitching moment growth effects, possibly also including the Küssner-effect. In this way the time-delay concept could also be used to effectively model the lift and moment growth of, for example a tailless aeroplane with wing sweep.

Before describing the penetration effect by a pure time-delay and by the two approximations (first order Padé and linear time derivative approximations) a remark should be made concerning the stability of a system containing one or more time-delays.

To compute the variance of output signals of a system by frequency-domain techniques, the system should be stable. In Ref. 19 it is remarked firstly that assessing the stability of a system incorporating one or more time-delays, can be a difficult and complicated matter. This is being dealt with in Ref. 20.

Secondly it is shown in Ref. 19 that a system incorporating one or more of the usual approximations of the time-delay may be stable whereas its original counterpart having the pure time-delays is unstable.

It should be noted that the remarks made are only relevant if the time-delays are incorporated in the system itself. For an aircraft this would be the case where the time-delay effect in still air (caused by a change of angle of attack of the aircraft itself) is described by a pure time-delay.
If this effect is described by the usual stability derivatives $C_{Z_{\dot{\alpha}}}$ and $C_{m_{\dot{\alpha}}}$ as in the computations of this Report, the system as such does not contain any time-delay. In fact there are two input signals, i.e. to the wing and to the tail, separated by a time-delay τ, as will be described in more detail below.

3.2. Description by a pure time-delay

In order to express the forces and moments due to vertical turbulence using the conventional gust derivatives such as $C_{Z_{\alpha_g}}$, $C_{m_{\alpha_g}}$, $C_{Z_{\dot{\alpha}_g}}$ and $C_{m_{\dot{\alpha}_g}}$, the change in angle of attack $\alpha_h(t)$ due to a gust $\alpha_g(t)$ at the aircraft's c.g. is considered as the sum of an instantaneous change in angle of attack of the horizontal tail

$$\alpha_g(t)\left(1 - \frac{d\varepsilon}{d\alpha}\right)$$

and a change $\Delta\alpha_h(t)$ caused by the penetration effect:

$$\alpha_h(t) = \alpha_g(t) \left(1 - \frac{d\varepsilon}{d\alpha}\right) + \Delta\alpha_h(t) \tag{8}$$

Thus the total change C_{Z_g} in normal force due to vertical turbulence is:

$$C_{Z_g} = C_{Z_{w_\alpha}} \cdot \alpha_g(t) + C_{Z_{h_\alpha}} \left(\frac{V_h}{V}\right)^2 \frac{S_h}{S} \cdot \left\{\alpha_g(t) \left(1 - \frac{d\varepsilon}{d\alpha}\right) + \Delta\alpha_h(t)\right\}$$

$$= C_{Z_{\alpha_g}} \cdot \alpha_g(t) + C_{Z_{h_\alpha}} \left(\frac{V_h}{V}\right)^2 \frac{S_h}{S} \cdot \Delta\alpha_h(t) \tag{9}$$

where:

$$C_{Z_{\alpha_g}} = C_{Z_{w_\alpha}} + C_{Z_{h_\alpha}} \cdot \left(\frac{V_h}{V}\right)^2 \frac{S_h}{S} \left(1 - \frac{d\varepsilon}{d\alpha}\right)$$

A similar expression holds for the pitching moment C_{m_g} due to vertical turbulence:

$$C_{m_g} = C_{m_{\alpha_g}} \cdot \alpha_g(t) + C_{Z_{h_\alpha}} \left(\frac{V_h}{V}\right)^2 \cdot \frac{S_h l_h}{S \cdot \bar{c}} \cdot \Delta\alpha_h(t) \tag{10}$$

The obvious advantage of this way of expressing C_{Z_g} and C_{m_g} is that in eqs. (9) and (10) the gust derivatives $C_{Z_{\alpha_g}}$ and $C_{m_{\alpha_g}}$ are identical with C_{Z_α} and C_{m_α} respectively, see Ref. 8.

In order to derive an expression for $\Delta\alpha_h(t)$ the change in angle of attack of the horizontal tail due to a gust $\alpha_g(t)$ at the aircraft's c.g. is again considered. As a result of the downwash, expressed by $\frac{d\varepsilon}{d\alpha}$ and of the time $\tau = \frac{l_h}{V}$ elapsed before the effect of the gust reaches the horizontal tail, its change in angle of attack can be written as:

$$\alpha_h(t) = \alpha_g\ (t-\tau) - \frac{d\varepsilon}{d\alpha}\,\alpha_g\ (t-\tau) = \left(1 - \frac{d\varepsilon}{d\alpha}\right)\alpha_g\ (t-\tau) \qquad (11)$$

From eqs. (8) and (11) it follows:

$$\Delta\alpha_h(t) = \left(1 - \frac{d\varepsilon}{d\alpha}\right)\left\{\alpha_g\ (t-\tau) - \alpha_g(t)\right\}$$

Using the transfer function $H(\omega)$ of a pure time-delay, relating input and output signals in the frequency domain:

$$H(\omega) = e^{-j\omega\tau}$$

the transfer function relating $\Delta\alpha_h(\omega)$ and $\alpha_g(\omega)$ becomes:

$$\frac{\Delta\alpha_h(\omega)}{\alpha_g(\omega)} = \left(1 - \frac{d\varepsilon}{d\alpha}\right)\left(e^{-j\omega\tau} - 1\right) \qquad (12)$$

3.3. First order Padé approximation

The transfer function of a pure time-delay is often approximated by (see Ref. 19):

$$H(\omega) = e^{-j\omega\tau} \approx \frac{1 - j\omega\tau/2}{1 + j\omega\tau/2}$$

Replacing $e^{-j\omega\tau}$ in eq. (12) by $H(\omega)$ according to the above approximation yields:

$$\frac{\Delta\alpha_h(\omega)}{\alpha_g(\omega)} = \left(1 - \frac{d\varepsilon}{d\alpha}\right)\left(\frac{1 - j\omega\tau/2}{1 + j\omega\tau/2} - 1\right) = -\left(1 - \frac{d\varepsilon}{d\alpha}\right) \cdot \frac{j\omega\tau}{1 + j\omega\tau/2} \qquad (13)$$

3.4. Linear time-derivative approximation (Truncated Taylor series)

Here the variable $\alpha_g(t - \tau)$ is approximated by the first two linear terms of a Taylor series:

$$\alpha_h(t) = \left(1 - \frac{d\varepsilon}{d\alpha}\right) \left\{\alpha_g(t) - \tau\dot{\alpha}_g(t)\right\}$$

Hence:

$$\Delta\alpha_h(t) = - \left(1 - \frac{d\varepsilon}{d\alpha}\right) \tau\dot{\alpha}_g(t)$$

The transfer function $\frac{\Delta\alpha_h(\omega)}{\alpha_g(\omega)}$ turns out to be that of a pure differentiator, multiplied by $- \left(1 - \frac{d\varepsilon}{d\alpha}\right) \tau$:

$$\frac{\Delta\alpha_h(\omega)}{\alpha_g(\omega)} = - \left(1 - \frac{d\varepsilon}{d\alpha}\right) . j\omega\tau \qquad (14)$$

Next the change of the normal force due to vertical turbulence according to eq. (9) is again considered and a new variable α_h' is introduced:

$$\alpha_h'(t) = - \frac{\bar{c}}{l_h} . \frac{1}{1 - \frac{d\varepsilon}{d\alpha}} . \Delta\alpha_h(t) \qquad (15)$$

It can be seen from eqs. (15) and (14), that, as $\tau = \frac{l_h}{V}$, α_h' becomes in the case of the linear time-derivative approximation:

$$\alpha_h'(t) = \dot{\alpha}_g(t) \frac{\bar{c}}{V} = D_c\alpha_g(t)$$

The introduction of α_h' allows the change in normal force to be written, using the gust derivative $C_{Z_{\dot{\alpha}_g}}$ (see Ref. 8), as:

$$C_{Z_g}(t) = C_{Z_{\alpha_g}} . \alpha_g(t) - \left(1 - \frac{d\varepsilon}{d\alpha}\right) C_{Z_{h_\alpha}} \left(\frac{V_h}{V}\right)^2 \frac{S_h l_h}{S \cdot \bar{c}} \alpha_h'(t)$$

$$= C_{Z_{\alpha_g}} . \alpha_g(t) + C_{Z_{\dot{\alpha}_g}} . \alpha_h'(t)$$

where:

$$C_{Z_{\dot{\alpha}_g}} = C_{Z_{\dot{\alpha}}} - C_{Z_q}$$

Similarly, the change in pitching moment becomes:

$$C_{m_g} = C_{m_{\alpha_g}} . \alpha_g(t) + C_{m_{\dot{\alpha}_g}} . \alpha_h'(t)$$

where:

$$C_{m_{\dot{\alpha}_g}} = C_{m_{\dot{\alpha}}} - C_{m_q}$$

Summarizing, the transfer functions relating $\alpha_h'(\omega)$ and $\alpha_g(\omega)$ for the pure time-delay, the first order Padé approximation and the linear time-derivative approximation are respectively:

$$H_{o_1}(\omega) = \frac{\alpha_h'(\omega)}{\alpha_g(\omega)} = -\frac{\bar{c}}{l_h} \cdot \left(e^{-j\omega\tau} - 1\right) \tag{16}$$

$$H_{o_2}(\omega) = \frac{\alpha_h'(\omega)}{\alpha_g(\omega)} = \frac{\bar{c}}{l_h} \cdot \frac{j\omega\tau}{1 + j\omega\tau/2} \tag{17}$$

$$H_{o_3}(\omega) = \frac{\alpha_h'(\omega)}{\alpha_g(\omega)} = \frac{D_g \alpha_g(\omega)}{\alpha_g(\omega)} = \frac{\bar{c}}{l_h} \cdot j\omega\tau \qquad (18)$$

Using the above definitions of $H_{o_1}(\omega)$, $H_{o_2}(\omega)$ and $H_{o_3}(\omega)$ the aircraft as perturbed by vertical turbulence may be represented by the block diagram of Fig. 2, where $H_1(\omega)$ and $H_2(\omega)$ are the aircraft's transfer functions relating an output signal x_u, for instance the normal acceleration, and the input signals α_g and α_h' respectively.

It is evident that $H_{o_1}(\omega)$ and $H_{o_2}(\omega)$ according to eqs. (16) and (17) will permit a computation of σ_n^2 in the frequency domain as the variable $D_c\alpha_g$, the one with an infinite variance, completely disappears from the aircraft's differential equations. For a computation in the time-domain according to the method described in Ref. 4 only the Padé approximation can be used.

4. POWER SPECTRAL DENSITIES OF THE NORMAL ACCELERATION, THE ANGLE OF ATTACK AND THE PITCHING VELOCITY

4.1. Normal acceleration at the aircraft's c.g.

In order to compare the three different ways of describing the penetration effect as presented in the third Chapter, the resulting power spectra of the normal acceleration factor caused by vertical turbulence have been calculated for an example aircraft under the assumption of constant speed. Particulars of the aircraft, a current subsonic four-engined jet transport in the approach configuration, are given in Table 5 at the end of this Report, together with the intensity and scale length of the vertical turbulence.
The intensity and scale length are those at a height of 265 m in a neutral atmosphere, according to the atmospheric model by Pritchard (see Ref. 2) for a reported wind speed of 0,5 m/sec (1 knot approx.) at 9,15 m altitude (30 ft), the terrain factor bein $R_T = 1,1$.

Referring to the block-diagram of Fig. 2, the resulting transfer function, denoted by the subscript r, and related to the entire system in the dashed lines of Fig. 2 is:

$$(H_{n\alpha_g})_r(\omega) = H_1(\omega) + H_o(\omega) \cdot H_2(\omega)$$

Hence the power spectrum of n can be written as:

$$\Phi_{nn}(\omega) = \left|(H_{n\alpha_g})_r(\omega)\right|^2 \cdot \Phi_{\alpha_g\alpha_g}(\omega)$$

$$= \{|H_1(\omega)|^2 + |H_2(\omega)|^2 \cdot |H_o(\omega)|^2 + H_1(\omega) \cdot H_2^*(\omega) \cdot H_o^*(\omega) +$$

$$+ H_1^*(\omega) \cdot H_2(\omega) \cdot H_o(\omega)\} \cdot \Phi_{\alpha_g\alpha_g}(\omega) \qquad (19)$$

where * denotes the complex conjugate. In Appendix 2 the transfer functions $H_1(\omega)$ and $H_2(\omega)$ are given.
Fig. 3 shows the Dryden power spectrum of α_g, Fig. 4 the moduli squared of the tranfer functions $H_{n\alpha_g}(\omega)$ resulting from $H_o(\omega)$ according to eqs. (16), (17) and (18).

The periodic nature of the modulus squared of the pure time-delay is caused by, see eq. (16):

$$|H_{o_1}(\omega)|^2 = 2\left(\frac{\bar{c}}{l_h}\right)^2 . (1 - \cos \omega\tau)$$

Fig. 5 gives the calculated power spectra of n. It can be seen from Figs. 4 and 5 that the Padé description is in good agreement with the pure time-delay whereas the first-order time derivative approximation, briefly to be called $D_c\alpha_g$-approximation, deviates markedly for high frequences. Fig. 5 clearly shows that the power spectrum of n for the $D_c\alpha_g$-approximation tends to the horizontal for high frequencies. Consequently a calculation of σ_n^2 by integrating $\Phi_{nn}(\omega)$ would yield an infinite value. This is not the case when $C_{Z_{\dot{\alpha}_g}}$ is set to zero, as can be seen from Figs. 4 and 5. Also shown in Figs. 4 and 5 are the modulus squared and the power spectrum for the case where the penetration effect is neglected ($C_{Z_{\dot{\alpha}_g}} = C_{m_{\dot{\alpha}_g}} = 0$).

In order to evaluate the different approximations, the power spectra of Fig. 5 have been numerically integrated to obtain the variance of n according to:

$$\sigma_n^2 = \int_0^{\omega_e} \Phi_{nn}(\omega) . d\omega \qquad (20)$$

The upper boundary ω_e was chosen at a sufficiently large value (ω_e = 100 rad/sec) to ensure a reasonable estimate of σ_n^2 to be obtained. The

results of this calculation are given in Table 1 below. For comparison the computed variance obtained by setting $C_{Z_{\dot{\alpha}_g}}$ and $C_{m_{\dot{\alpha}_g}}$ to zero i.e. by neglecting the penetration effect altogether, is also presented in the Table.

Table 1. Variance of normal acceleration (g^2)

	V = const. $C_{Z_{\dot{\alpha}_g}} \neq 0$	V = const. $C_{Z_{\dot{\alpha}_g}} = 0$	V = var.
Time lag	1.95×10^{-4}	2.13×10^{-4}	-
Padé approx.	1.96×10^{-4}	2.13×10^{-4}	1.97×10^{-4}
$D_c\alpha_g$ approx. (ω_e = 100 rad/sec)	2.96×10^{-4}	2.26×10^{-4}	-
No pen. effect	1.67×10^{-4}	-	-

From this Table, several conclusions may be drawn. Firstly it appears that a first order Padé filter yields, for this catagory of calculations, a very good approximation of the pure time-delay. Secondly it can be seen that setting $C_{Z_{\dot{\alpha}_g}}$ to zero yields an error of up to 15% approximately Finally it can be concluded that neglecting the penetration effect is hardly permissable.

In order to extrapolate these conclusions to the case of unrestricted aircraft motions (variable speed), a calculation of σ_n^2 for the unrestricted aircraft, using the Padé approximation, was performed by the method described in Ref. 11. The result, included in Table 1 under the heading "V = var." affirms the well know fact that the aircraft's normal acceleration due to vertical turbulence can very accurately be

approximated by assuming constant speed.

In the introduction it was stated that in the case of an analogue Monte Carlo simulation the variance of n will, also in the case of the $D_c\alpha_g$-approximation, always be finite due to the limited bandwidth of electronic white noise generators. As can be seen from Fig. 5, the result of such a simulation would, in a rather unexpected way, be dependent on the cut-off frequency of the noise generator, as the error in the computed variance would increase with increasing cut-off frequency.

In Table 1 the result is given of a digital integration up to a frequency of ω_e = 100 rad/sec (16 Hz approximately) for the $D_c\alpha_g$-approximation. The result can be considered as representative of a Monte Carlo simulation using a white noise filter with a cut-off frequency of about 16 Hz. The result is in error as much as 50% and would be more so in the case of higher cut-off frequencies.

4.2. Normal acceleration in arbitrary points of the aircraft

According to eq. (4) the normal acceleration in a point $x - x_{c.g.}$ aft of the aircraft's c.g. is:

$$n_x = n_{c.g.} - \frac{V}{g} \frac{x - x_{c.g.}}{\bar{c}} \cdot \frac{\dot{q}\bar{c}}{V} \tag{21}$$

A computation of the variance of n_x can be performed by considering n_x as the sum in the right had part of (21), see the block-diagram of Fig. 6. The power spectral density of n_x is then:

$$\Phi_{n_x n_x}(\omega) = \{|H_I(\omega)|^2 + |H_{II}(\omega)|^2 + H_I(\omega) \cdot H_{II}^*(\omega) +$$

$$+ H_I^*(\omega)\, H_{II}(\omega)\} \cdot \Phi_{\alpha_g \alpha_g}(\omega) \tag{22}$$

where:

$$H_I(\omega) = (H_{n\alpha_g})_r(\omega) = H_1(\omega) + H_o(\omega) \cdot H_2(\omega)$$

$$H_{II}(\omega) = -\frac{V}{g} \cdot \frac{x - x_{c.g.}}{\bar{c}} \cdot (H_{\dot{q}\alpha_g})_r(\omega) =$$

$$= -\frac{V}{g} \cdot \frac{x - x_{c.g.}}{\bar{c}} \cdot \{H_3(\omega) + H_o(\omega) \cdot H_4(\omega)\}$$

The transfer functions $H_3(\omega)$ and $H_4(\omega)$ are given in Appendix 2. The variance $\sigma^2_{n_x}$ can again be computed by integrating the power spectrum according to eq. (22) in the frequency domain:

$$\sigma^2_{n_x} = \int_0^\infty \Phi_{n_x n_x}(\omega) \cdot d\omega \tag{23}$$

As the variance $\sigma_y^{\,2}$ of a linear function $y(x,z) = ax + bz$ is given by:

$$\sigma_y^{\,2} = a^2 . \sigma_x^{\,2} + b^2 . \sigma_z^{\,2} + 2ab . \sigma_{xz}$$

the variance of n_x can be written as, see eq. (21):

$$\sigma^2_{n_x} = \sigma^2_{n_{c.g.}} + \frac{V^2}{g^2}\left(\frac{x - x_{c.g.}}{\bar{c}}\right)^2 \cdot \sigma_{\dot{q}}^{\,2} - \frac{2V}{g} \cdot \frac{x - x_{c.g.}}{\bar{c}} \cdot \sigma_{n\dot{q}} \tag{24}$$

where $\sigma_{\dot{q}}^{\,2}$ is the variance of $\frac{\dot{q}\bar{c}}{V}$ and $\sigma_{n_{\dot{q}}}$ is the covariance of $n_{c.g.}$ and $\frac{\dot{q}\bar{c}}{V}$, it follows from eqs. (23) and (24) that:

$$\int_0^\infty \{H_I(\omega)' . H_{II}^{\ *}(\omega) + H_I^{\ *}(\omega) . H_{II}(\omega)\} \Phi_{\alpha_g\alpha_g} . d\omega =$$

$$= - \frac{2V}{g} \cdot \frac{x - x_{c.g.}}{\bar{c}} \cdot \sigma_{n\dot{q}} \qquad (25)$$

and

$$\int_0^\infty |H_{II}(\omega)|^2 \cdot \Phi_{\alpha_g\alpha_g}(\omega) \cdot d\omega = \left(\frac{V}{g}\right)^2 \left(\frac{x - x_{c.g.}}{\bar{c}}\right)^2 \cdot \sigma_{\dot{q}}^2 \qquad (26)$$

As $H_3(\omega) \cdot H_{II}^*(\omega)$ and $H_I^*(\omega) \cdot H_{II}(\omega)$ are complex conjugate functions it is easily shown that:

$$H_I(\omega) \cdot H_{II}^*(\omega) \cdot \Phi_{\alpha_g\alpha_g}(\omega) = - \frac{V}{g} \cdot \frac{x - x_{c.g.}}{\bar{c}} \cdot \sigma_{\dot{q}n}(\omega) \qquad (27a)$$

and

$$H_I^*(\omega) \cdot H_{II}(\omega) \cdot \Phi_{\alpha_g\alpha_g}(\omega) = - \frac{V}{g} \cdot \frac{x - x_{c.g.}}{\bar{c}} \cdot \sigma_{n\dot{q}}(\omega) \qquad (27b)$$

Moreover, of course:

$$|H_{II}(\omega)|^2 \cdot \Phi_{\alpha_g\alpha_g}(\omega) = \left(\frac{V}{g}\right)^2 \cdot \left(\frac{x - x_{c.g.}}{\bar{c}}\right)^2 \cdot \sigma_{\dot{q}\dot{q}}(\omega) \qquad (28)$$

where $\Phi_{\dot{q}\dot{q}}(\omega)$ denotes the power spectrum of $\frac{\dot{q}\bar{c}}{V}$.

In order to gain some insight into the contributions of $\sigma_{\dot{q}}^2$ and $\sigma_{n\dot{q}}$ to $\sigma_{n_x}^2$ (see eq. (24)), the power spectrum of $\frac{\dot{q}\bar{c}}{V}$ and the cross spectrum of $n_{c.g.}$ and $\frac{\dot{q}\bar{c}}{V}$ have been calculated for the example aeroplane, again assuming constant speed.

Figures 7 and 8 show the moduli squared of the transfer functions $H_{\dot{q}\alpha_g}(\omega)$

and the power-spectra of $\frac{\dot{q}\bar{c}}{V}$, according to the several descriptions. Again the Padé approximation is in rather good agreement with the pure time-lag, while the spectrum of $\frac{\dot{q}\bar{c}}{V}$ resulting from the $D_c\alpha_g$ approximation tends to the horizontal for frequencies higher than 1 rad/sec. Neglecting the penetration effect ($C_{m_{\dot{\alpha}_g}} = C_{Z_{\dot{\alpha}_g}} = 0$) causes a spectrum too high at low frequencies and to low at high frequencies. Table 2 gives the result of the digital integration of the power spectra, together with the result of the digital calculation mentioned before for the unrestricted aircraft (V = var.).

Table 2. Variance of $\frac{\dot{q}\bar{c}}{V}$ (rad^2 sec^{-2})

	V = const.	V = var.
Time lag	6.14×10^{-8}	
Padé approx.	5.97×10^{-8}	5.70×10^{-8}
$D_c\alpha_g$ approx. (ω_e = 100 rad/sec)	71.45×10^{-8}	
No pen. effect	0.858×10^{-8}	

Some insight into the next contribution to $\sigma^2_{n_x}$ according to eq. (24), i.e. the contribution of $\sigma_{n\dot{q}}$, can be gained by observing the cross spectru $\Phi_{n\dot{q}}(\omega)$, the real part of which is plotted in Fig. 9. The imaginary part i not shown as it does not yield a contribution to $\sigma^2_{n_x}$.

Integrating the real part of $\Phi_{n\dot{q}}(\omega)$ for the $D_c\alpha_g$ approximation from $\omega = 0$ to $\omega = \infty$ would result in an infinite covariance $\sigma_{n\dot{q}}$. The results of the numerical integration are summarized in Table 3, together with the result for the case of variable speed (V = var.).

Table 3. Covariance of n and $\frac{\dot{q}\bar{c}}{V}$ (g rad sec^{-1})

	V = const.	V = var.
Time lag	-0.59×10^{-6}	-
Padé approx.	-0.59×10^{-6}	-0.56×10^{-6}
$D_c\alpha_g$ approx. (ω_e = 100 rad/sec)	-8.35×10^{-6}	-
No pen. effect	-1.12×10^{-6}	-

In Tables 2 and 3 again the result for the $D_c\alpha_g$-approximation is given for an upper boundary of integration of ω_e = 100 rad/sec. It will be evident that the remarks in the foregoing paragraph on the results of a Monte Carlo simulation can also be made for the variance of $\frac{\dot{q}\bar{c}}{V}$, the covariance of $n_{c.g.}$ and $\frac{\dot{q}\bar{c}}{V}$ and finally, of course, for the resulting variance of n_x, as will be shown in the next chapter.

4.3. The angle of attack and the pitching velocity

In the foregoing it was shown that a Padé approximation yielded results in good agreement with those obtained by a pure time delay description in the case of a calculation of the variance of the normal acceleration.

Now the question arises

a) whether this will also be so in the case of other motion variables where the $D_c\alpha_g$ approximation is theoretically possible and
b) how the results of the $D_c\alpha_g$ approximation will compare with those of the time delay and the Padé description.

Therefore the power spectra of the two relevant motion variables in the case of constant speed, see Appendix 1, i.e. the angle of attack α and the dimensionless pitching velocity $\frac{qc}{V}$ have been calculated and integrated numerically to obtain the variances σ_α^2 and $\sigma^2_{\frac{q\bar{c}}{V}}$.

The power spectra of α and $\frac{q\bar{c}}{V}$ are shown in Figs. 10 and 11 respectively. It is evident that for both motion variables the Padé approximation is in good agreement with the time delay. For the angle of attack the $D_c\alpha_g$ spectrum is very close to the power spectrum resulting from time delay and Padé description. However, the power spectrum for $\frac{q\bar{c}}{V}$ in the case of the $D_c\alpha_g$ description is higher for all frequencies (Fig. 11) and a larger variance is found as can be seen from Table 4.

Table 4. Variance of angle of attack α and pitching velocity $\frac{q\bar{c}}{V}$

	σ_α^2 (rad^2)	$\sigma^2_{\frac{q\bar{c}}{V}}$ (rad^2)
Time lag	8.11×10^{-6}	0.663×10^{-8}
Padé approx.	8.12×10^{-6}	0.636×10^{-8}
$D_c\alpha_g$ approx.	8.48×10^{-6}	0.919×10^{-8}

It can be seen from Table 4 that the r.m.s. value of $\frac{q\bar{c}}{V}$ as obtained by the $D_c\alpha_g$ approximation is in error approximately 20% if compared with the time delay result.

5. THE VARIANCE OF THE NORMAL ACCELERATION AS A FUNCTION OF $\frac{x - x_{c.g.}}{\bar{c}}$. SOME NUMERICAL EXAMPLES

One example of the power-spectrum of n_x has been calculated and is shown in Fig. 12. The location of $\frac{x - x_{c.g.}}{\bar{c}} = 3$ roughly corresponds with that of the horizontal tail.

Using the results given in Tables 1, 2 and 3 the variance of n_x as a function of the location along the aircraft's X-axis has been calculated by using eq. (24).
The results of the pure time delay and those of the Padé approximation only differ slightly and only the Padé and $D_c\alpha_g$ results have been plotted in Fig.13, together with the results obtained by neglecting the penetration effect.

As can be observed from Tables 1, 2 and 3, the Padé curves in Fig. 13 for constant and variable flight speed are so close as to coïncide and it can be concluded that the assumption of constant speed is also valid for the computation of the normal acceleration at arbitrary points in the aircraft.

Neglecting the penetration effect would underestimate the variance of n_x, especially at the most forward locations. Due to the overestimated variance of $\frac{\dot{q}\bar{c}}{V}$ by the $D_c\alpha_g$-approximation (see Table 2) the computed normal acceleration variance in points at some distance from the c.g. is too large.

Finally the variance of n_x has been calculated, under the assumption of constant speed, for two more example aircraft, again for the case of vertical turbulence only.

Particulars of the aircraft are given in Table 6 at the end of this Report, the results are given in Fig. 14.
Aircraft type A is the one used throughout in this Report. Type B is a four-engined, type A a twin engined propeller transport, both in cruising

flight. Especially in type C, the variance of n_x is strongly dependent on the location in the aircraft, while apparently the covariance of $n_{c.g.}$ and $\frac{\dot{q}\bar{c}}{V}$ is very small; this covariance is larger in the case of aircraft B.

Obviously the relatively large moment of inertia of type A, which is of a rear-engined configuration, prevents the aeroplane from acquiring high pitching accelerations.

The marked tendency of the curves in Fig. 14 to have a positive slope is due to a negative value of $\sigma_{n\dot{q}}$ (see eq. (24)). This can roughly be explained by the fact that a stable aeroplane has a tendency to pitch down (negative pitching moment) when hit by an upward gust which causes a positive normal acceleration, and vice versa.

6. CONCLUSIONS

It was shown that a theoretical calculation of the variance if the aircraft's normal acceleration due to atmosperhic turbulence is not possible if the linear time derivative approximation of the gust penetration effect is used in conjunction with the Dryden or von Karman turbulence power spectral densities.

Neglecting the derivative $C_{Z_{\dot{\alpha}_g}}$ allows an approximate calculation of the normal acceleration at the aircraft's c.g. to be made. Neglecting the penetration effect altogether (point approximation of the turbulent field) may cause large errors in the normal acceleration, especially at points at some distance from the aircraft's c.g., when compared with results obtained by a pure time-delay description of the penetration effect.

It was shown that a first order Padé description yields results in very good agreement with those obtained by a pure time-delay.

In the case of the linear time derivative approximation of the gust penetration effect, the results of a calculation of the normal acceleration variance, which was theoretically shown to be infinite in this case, would, obtained by an analogue Monte Carlo simulation, misleadingly, be finite. This is due to the limited bandwidth of electronic noise generators.
The variance thus calculated may be much too large, and more so for higher cut-off frequences of the white noise generator.

7. REFERENCES

1) B. Etkin — A theory of the response of airplanes to random atmospheric turbulence. Journal of the Aero/Space Sciences, Vol. 26, no. 7, July 1959, p. 409.

2) Approach and landing simulation. AGARD Report no. 632, 1975.

3) C.K. Gordon, R.O. Dodson — STOL Ride control feasibility study Technical Report. NASA CR-2276, 1973.

4) W.J. Oehman — Analytical study of the performance of a gust alleviation system for a STOL-airplane. NASA TN-D-7201, 1973.

5) R.L. Bisplinghoff, H. Ashley, R.L. Halfman — Aeroelasticity. Addison-Wesley Publishing Cy., Cambridge, Mass., USA, 1957.

6) B. Etkin — Dynamics of atmospheric flight. John Wiley & Sons Inc., New York - London - Sydney - Toronto, 1972.

7) L.K. Barker — Power-spectral-density relationship for retarded differential equations. NASA TN D-7761, 1974.

8) O.H. Gerlach — Calculation of the response of an aircraft to random atmospheric turbulence. Part I. Symmetric motions. Report VTH-138, Delft University of Technology, Department of Aeronautical Engineering, 1966.

9) J.C. van der Vaart — The cross-covariance of gust velocities and their time-derivatives.

Report VTH-207, Delft University of Technology, Department of Aerospace Engineering, 1975.

10) J.C. van der Vaart — The impulse response method for the calculation of statistical properties of an aircraft flying in random atmospheric turbulence. Report VTH-197, Delft University of Technology, Department of Aerospace Engineering, 1975.

11) H.L. Jonkers, F.K. Kappetijn, J.C. van der Vaart — Digital calculation of the propagation in time of the aircraft gust response covariance matrix. Report VTH- , Delft University of Technology, Department of Aerospace Engineering, to be published.

12) Y.P. Dobrolenskiy — Flight dynamics in moving air. (Dynamika Poleta v Nespokoynoy Atmosfere). NASA T.T. F-600, 1971.

13) W.L. Cowley, H. Glauert — The effect of the lag of the downwash on the longitudinal stability of an aeroplane on the rotary derivative M_q. R & M no. 718, 1921.

14) R.I. Jones, L.F. Fehlner — Transient effects of the wing wake on the horizontal tail. NACA TN-no. 771, 1940.

15) B. Mazelsky, F.W. Diederich — A method of determining the effect of airplane stability on the gust load factor. NACA TN-2035, 1950.

16) M. Tobak — On the use of the indicial function concept in the analysis of unsteady motions of wings and wing-tail combinations. NACA Report 1188, 1954.

17) F.W. Diederich — The response of an airplane to random atmospheric disturbances. NACA TN-3910, 1957.

18) F.O. Smetana, R.K. Carden — An analytical study of the response of a constant attitude aircraft to atmospheric turbulence. NASA CR-2204, 1973.

19) L.K. Barker — Power-spectral-density relationship for retarded differential equations. NASA TN-D-7761, 1974.

20) J.D. Shaughnessy, Y. Kashiwagi — The determination of a stability indicative function for linear systems with multiple delays. NASA TR.R-301, 1969.

Table 5. Data of example aircraft and vertical turbulence.

Aircraft type A: four-engined, subsonic jet transport, approach configuration.

W	$= 96160$ kg	V	$= 71{,}24$ m/sec
S	$= 260{,}68$ m^2	μ_{c_2}	$= 49{,}315$
$\bar{c}$	$= 6{,}10$ m	K_Y^2	$= 2{,}354$
b	$= 42{,}67$ m	h	$= 265$ m
$x_{c.g.}$	$= 0{,}36\ \bar{c}$		

C_{X_o}	$= -0{,}0507$	C_{Z_o}	$= -1{,}163$		
C_{X_u}	$= -0{,}370$	C_{Z_u}	$= -2{,}326$	C_{m_u}	$= 0$
C_{X_α}	$= 0{,}655$	C_{Z_α}	$= -5{,}04$	C_{m_α}	$= -0{,}72$
		$C_{Z_{\dot\alpha}}$	$= -0{,}395$	$C_{m_{\dot\alpha}}$	$= -1{,}218$
		C_{Z_q}	$= -4{,}65$	C_{m_q}	$= -8{,}622$
$C_{X_{\alpha_g}}$	$= 0{,}655$	$C_{Z_{\alpha_g}}$	$= -5{,}04$	$C_{m_{\alpha_g}}$	$= -0{,}72$
$C_{X_{\dot\alpha_g}}$	$= 0$	$C_{Z_{\dot\alpha_g}}$	$= 4{,}255$	$C_{m_{\dot\alpha_g}}$	$= 7{,}40$

Vertical turbulence

Dryden power spectral density:

$$\Phi_{\alpha_g\alpha_g}(\omega) = \frac{\sigma_{\alpha_g}^2}{\pi} \cdot \frac{L_g}{V} \cdot \frac{1 + 3\left(\omega \frac{L_g}{V}\right)^2}{\left\{1 + \left(\omega \frac{L_g}{V}\right)^2\right\}^2}$$

$L_g = 150$ m, $\sigma_{\alpha_g} = 0{,}00396$ rad $(\sigma_{w_g} = 0{,}282$ m/sec)

(Pritchard atmospheric model, see Ref. 2, $h = 265$ m, $V_{w_{9,15}} = 0{,}5$ m/sec, $R_T = 1{,}1$, neutral atmosphere.)

Table 6. Data of example aircraft B and C.

Aircraft type B: four-engined propeller transport, cruise configuration.

W = 59020 kg		V = 145 m/sec	
S = 153,5 m^2		μ_{c_2} = 144	
$\bar{c}$ = 4,47 m		K_Y^2 = 1.473	
b = 37,49 m		h = 6900 m	
C_{Z_o} = - 0,60			
C_{Z_α} = - 6,225	C_{m_α} = - 0,975		
$C_{Z_{\dot\alpha}}$ = - 1,420	$C_{m_{\dot\alpha}}$ = - 5,450		
C_{Z_q} = - 3,820	C_{m_q} = - 18,450		
$C_{Z_{\alpha_g}}$ = - 6,225	$C_{m_{\alpha_g}}$ = - 0,975		
$C_{Z_{\dot\alpha_g}}$ = 2,400	$C_{m_{\dot\alpha_g}}$ = 13,030		

Aircraft type C: twin-engined propeller transport, cruise configuration.

W = 16200 kg		V = 125,5 m/sec	
S = 70 m^2		μ_{c_2} = 137,5	
$\bar{c}$ = 2,58 m		K_Y^2 = 0,272	
b = 29,0 m		h = 6100 m	
C_{Z_o} = - 0,45			
C_{Z_α} = - 5,90	C_{m_α} = - 0,80		
$C_{Z_{\dot\alpha}}$ = - 1,59	$C_{m_{\dot\alpha}}$ = - 6,50		
C_{Z_q} = - 7,36	C_{m_q} = - 16,50		
$C_{Z_{\alpha_g}}$ = - 5,9	$C_{m_{\alpha_g}}$ = - 0,80		
$C_{Z_{\dot\alpha_g}}$ = 5,77	$C_{m_{\dot\alpha_g}}$ = 10,0		

APPENDIX 1. DIFFERENTIAL EQUATIONS FOR AN AIRCRAFT PERTURBED BY ATMOSPHERIC TURBULENCE

The linearized differential equations for the symmetrical motions due to turbulence are, if $\delta_e = 0$:

$$\begin{bmatrix} C_{X_u}-2\mu_c D_c & C_{X_\alpha} & C_{Z_o} & 0 \\ C_{Z_u} & C_{Z_\alpha}-(2\mu_c-C_{Z_{\dot\alpha}})D_c & -C_{X_o} & 2\mu_c+C_{Z_q} \\ 0 & 0 & -D_c & 1 \\ C_{m_u} & C_{m_\alpha}+C_{m_{\dot\alpha}}D_c & 0 & C_{m_q}-2\mu_c K_Y^2 D_c \end{bmatrix} \cdot \begin{bmatrix} \hat{u} \\ \alpha \\ \theta \\ \frac{q\bar{c}}{V} \end{bmatrix} =$$

$$- \begin{bmatrix} C_{X_{u_g}} & C_{X_{\dot u_g}} & C_{X_{\alpha_g}} & C_{X_{\dot\alpha_g}} \\ C_{Z_{u_g}} & C_{Z_{\dot u_g}} & C_{Z_{\alpha_g}} & C_{Z_{\dot\alpha_g}} \\ 0 & 0 & 0 & 0 \\ C_{m_{u_g}} & C_{m_{\dot u_g}} & C_{m_{\alpha_g}} & C_{m_{\dot\alpha_g}} \end{bmatrix} \cdot \begin{bmatrix} \hat{u}_g \\ D_c\hat{u}_g \\ \alpha_g \\ D_c\alpha_g \end{bmatrix} \qquad \text{(A1-1)}$$

The desired form of the system equation:

$$\dot{\bar{x}} = [A]\,\bar{x} + [B] \cdot \bar{y}_g$$

can be obtained by eliminating the term $C_{m_{\dot\alpha}} \cdot D_c\alpha$ in eq. (A1-1). This is done by multiplying the Z-equation of eq. (A-1) by $\frac{C_{m_\alpha}}{2\mu_c - C_{Z_{\dot\alpha}}}$, summing the result and the M-equation and finally deviding the X-equation by $2\mu_c$, the Z-equation by $2\mu_c - C_{Z_{\dot\alpha}}$ and the M-equation

by $2\mu_c \cdot K_Y^2$. The result is, in abbreviated notation

$$\begin{bmatrix} \dot{\hat{u}} \\ \dot{\alpha} \\ \dot{\theta} \\ \frac{\dot{q}\bar{c}}{V} \end{bmatrix} \cdot \frac{\bar{c}}{V} = \begin{bmatrix} x_u & x_\alpha & x_\theta & 0 \\ z_u & z_\alpha & z_\theta & z_q \\ 0 & 0 & 0 & 1 \\ m_u & m_\alpha & m_\theta & m_q \end{bmatrix} \cdot \begin{bmatrix} \hat{u} \\ \alpha \\ \theta \\ \frac{q\bar{c}}{V} \end{bmatrix} + \begin{bmatrix} x_{u_g} & x_{\dot{u}_g} & x_{\alpha_g} & x_{\dot{\alpha}_g} \\ z_{u_g} & z_{\dot{u}_g} & z_{\alpha_g} & z_{\dot{\alpha}_g} \\ 0 & 0 & 0 & 0 \\ m_{u_g} & m_{\dot{u}_g} & m_{\alpha_g} & m_{\dot{\alpha}_g} \end{bmatrix} \cdot \begin{bmatrix} \hat{u}_g \\ D_c\hat{u}_g \\ \alpha_g \\ D_c\alpha_g \end{bmatrix} \qquad \text{(A1-2)}$$

The coefficients in (A1-2) have the following meaning:

$$x_u = \frac{C_{X_u}}{2\mu_c} \qquad z_u = \frac{C_{Z_u}}{2\mu_c - C_{Z_{\dot{\alpha}}}} \qquad m_u = \frac{C_{m_u} + C_{Z_u} \cdot \frac{C_{m_{\dot{\alpha}}}}{2\mu_c - C_{Z_{\dot{\alpha}}}}}{2\mu_c K_Y^2}$$

$$x_\alpha = \frac{C_{X_\alpha}}{2\mu_c} \qquad z_\alpha = \frac{C_{Z_\alpha}}{2\mu_c - C_{Z_{\dot{\alpha}}}} \qquad m_\alpha = \frac{C_{m_\alpha} + C_{Z_\alpha} \cdot \frac{C_{m_{\dot{\alpha}}}}{2\mu_c - C_{Z_{\dot{\alpha}}}}}{2\mu_c K_Y^2}$$

$$x_\theta = \frac{C_{Z_o}}{2\mu_c} \qquad z_\theta = \frac{-C_{X_o}}{2\mu_c - C_{Z_{\dot{\alpha}}}} \qquad m_\theta = \frac{-C_{X_o} \cdot \frac{C_{m_{\dot{\alpha}}}}{2\mu_c - C_{Z_{\dot{\alpha}}}}}{2\mu_c K_Y^2}$$

$$z_q = \frac{2\mu_c + Cz_q}{2\mu_c - Cz_{\dot\alpha}} \qquad m_q = \frac{C_{m_q} + \dfrac{2\mu_c + Cz_q}{2\mu_c - Cz_{\dot\alpha}} \cdot C_{m_{\dot\alpha}}}{2\mu_c K_Y^2}$$

$$x_{u_g} = \frac{Cx_{u_g}}{2\mu_c} \qquad z_{u_g} = \frac{Cz_{u_g}}{2\mu_c - Cz_{\dot\alpha}} \qquad m_{u_g} = \frac{C_{m_{u_g}} + Cz_{u_g} \dfrac{C_{m_{\dot\alpha}}}{2\mu_c - Cz_{\dot\alpha}}}{2\mu_c K_Y^2}$$

$$x_{\dot u_g} = \frac{Cx_{\dot u_g}}{2\mu_c} \qquad z_{\dot u_g} = \frac{Cz_{\dot u_g}}{2\mu_c - Cz_{\dot\alpha}} \qquad m_{\dot u_g} = \frac{C_{m_{\dot u_g}} + Cz_{\dot u_g} \dfrac{C_{m_{\dot\alpha}}}{2\mu_c - Cz_{\dot\alpha}}}{2\mu_c K_Y^2}$$

$$x_{\alpha_g} = \frac{Cx_{\alpha_g}}{2\mu_c} \qquad z_{\alpha_g} = \frac{Cz_{\alpha_g}}{2\mu_c - Cz_{\dot\alpha}} \qquad m_{\alpha_g} = \frac{C_{m_{\alpha_g}} + Cz_{\alpha_g} \dfrac{C_{m_{\dot\alpha}}}{2\mu_c - Cz_{\dot\alpha}}}{2\mu_c K_Y^2}$$

$$x_{\dot\alpha_g} = \frac{Cx_{\dot\alpha_g}}{2\mu_c} \qquad z_{\dot\alpha_g} = \frac{Cz_{\dot\alpha_g}}{2\mu_c - Cz_{\dot\alpha}} \qquad m_{\dot\alpha_g} = \frac{C_{m_{\dot\alpha_g}} + Cz_{\dot\alpha_g} \dfrac{C_{m_{\dot\alpha}}}{2\mu_c - Cz_{\dot\alpha}}}{2\mu_c K_Y^2}$$

Under the assumption of constant speed ($\hat{u} = 0$), the X-equation in (A1-2) disappears. If the steady flight condition, relative to which perturbations are considered, is a horizontal or nearly horizontal flight, Cx_o may be set to zero, which means $z_\theta = m_\theta = 0$. If the variable θ is further neglected as a separate motion variable, the differential equations now become, if only vertical turbulence is considered:

$$\begin{bmatrix} \dot\alpha \\ \dfrac{\dot q \bar c}{V} \end{bmatrix} \cdot \frac{\bar c}{V} = \begin{bmatrix} z_\alpha & z_q \\ m_\alpha & m_q \end{bmatrix} \cdot \begin{bmatrix} \alpha \\ \dfrac{q\bar c}{V} \end{bmatrix} + \begin{bmatrix} z_{\alpha_g} & z_{\dot\alpha_g} \\ m_{\alpha_g} & m_{\dot\alpha_g} \end{bmatrix} \cdot \begin{bmatrix} \alpha_g \\ D_c \alpha_g \end{bmatrix} \qquad \text{(A1-3)}$$

By multiplying eq. (A1-3) by $\frac{V}{\bar{c}}$, the system equation:

$$\dot{\bar{x}} = [A]\,\bar{x} + [B]\,.\,\bar{y}_g \qquad \text{(A1-4)}$$

is obtained, where:

$$\bar{x} = \begin{bmatrix} \alpha \\ \frac{\bar{q}\bar{c}}{V} \end{bmatrix}, \quad [A] = \begin{bmatrix} z_\alpha & z_q \\ m_\alpha & m_q \end{bmatrix} \cdot \frac{V}{\bar{c}}, \quad [B] = \begin{bmatrix} z_{\alpha_g} & z_{\dot{\alpha}_g} \\ m_{\alpha_g} & m_{\dot{\alpha}_g} \end{bmatrix} \cdot \frac{V}{\bar{c}}$$

and

$$\bar{y}_g = \begin{bmatrix} \alpha_g \\ D_c\alpha_g \end{bmatrix}$$

It will be evident from Chapter 3 that $D_c\alpha_g$ may be replaced by α_h' in the case of a pure time-delay or a first order Padé description of the penetration effect.

APPENDIX 2. TRANSFER FUNCTIONS FOR THE NORMAL ACCELERATION DUE TO VERTICAL TURBULENCE UNDER THE ASSUMPTION OF CONSTANT SPEED

The matrix [H(P)] of the transfer function relating $\alpha(P)$ and $\frac{\bar{qc}}{V}(P)$ to $\alpha_g(P)$ and $D_c\alpha_g(P)$ or $\alpha_h(P)$, where P is the complex Laplace variable, is obtained from eq. (A1-4) by (see Ref. 6):

$$[H(P)] = [R(P)]^{-1} \cdot [B] \tag{A2-1}$$

where:

$$[R] = P[I] - [A]$$

and [I] is the unit matrix. In this way the following transfer functions can be derived:

$$H_{\alpha\alpha_g}(P) = \frac{\alpha(P)}{\alpha_g(P)}$$

$$H_{q\alpha_g}(P) = \frac{\frac{\bar{qc}}{V}(P)}{\alpha_g(P)} \tag{A2-2}$$

$$H_{\alpha\alpha_h'}(P) = \frac{\alpha(P)}{\alpha_h'(P)}$$

$$H_{q\alpha_h'}(P) = \frac{\frac{\bar{qc}}{V}(P)}{\alpha_h'(P)}$$

The normal acceleration factor at the aircraft's c.g. is:

$$n_{c.g.} = \frac{V^2}{g\bar{c}} \left(\frac{\dot{\theta}\bar{c}}{V} - \frac{\dot{\alpha}\bar{c}}{V} \right) = \frac{V^2}{g\bar{c}} \left(\frac{q\bar{c}}{V} - \frac{\dot{\alpha}\bar{c}}{V} \right)$$

The transfer functions relating $\frac{\dot{\alpha}\bar{c}}{V}(P)$ to $\alpha_g(P)$ and $\alpha_h'(P)$ are easily obtained by:

$$H_{\dot{\alpha}\alpha_g}(P) = \frac{\frac{\dot{\alpha}\bar{c}}{V}(P)}{\alpha_g(P)} = \frac{\bar{c}}{V} \cdot P \cdot H_{\alpha\alpha_g}(P)$$

$$H_{\dot{\alpha}\alpha_h'}(P) = \frac{\frac{\dot{\alpha}\bar{c}}{V}(P)}{\alpha_h'(P)} = \frac{\bar{c}}{V} \cdot P \cdot H_{\alpha\alpha_h'}(P) \qquad \text{(A2-3)}$$

Referring to the block-diagram of Fig. 2, the resulting transfer function relating the normal acceleration to the input signal of the entire system in the dashed lines, is:

$$H_I(\omega) = (H_{n\alpha_g})_r (P) = H_1(P) + H_o(P) \cdot H_2(P)$$

where:

$$H_1(P) = \frac{V^2}{g\bar{c}} \left\{ \frac{\frac{q\bar{c}}{V}(P)}{\alpha_g(P)} - \frac{\frac{\dot{\alpha}\bar{c}}{V}(P)}{\alpha_g(P)} \right\}$$

$$H_2(P) = \frac{V^2}{g\bar{c}} \left\{ \frac{\frac{q\bar{c}}{V}(P)}{\alpha_h'(P)} - \frac{\frac{\dot{\alpha}\bar{c}}{V}(P)}{\alpha_h'(P)} \right\}$$

The tranfer functions $H_1(P)$ and $H_2(P)$ can be derived using eqs. (A2-1), (A2-2) and (A2-3). The result is:

$$H_1(P) = \frac{b_{n_2} P^2 + b_{n_1} P + b_{n_o}}{P^2 + a_1 P + a_o}$$

$$H_2(P) = \frac{b_{n_2}' P^2 + b_{n_1}' P + b_{n_o}}{P^2 + a_1 P + a_o}$$

where:

$$a_1 = - \frac{V}{c} \cdot (z_\alpha + m_q)$$

$$a_o = \frac{V}{c} (z_\alpha m_q - m_\alpha z_q)$$

$$b_{n_2} = - \frac{V^2}{gc} \cdot z_{\alpha_g}$$

$$b_{n_1} = \frac{V^2}{gc} \cdot (z_{\alpha_g} \cdot m_q - m_{\alpha_g} z_q + \frac{V}{c} \cdot m_{\alpha_g})$$

$$b_{n_o} = - \frac{V^2}{gc} (z_\alpha m_{\alpha_g} - m_\alpha z_{\alpha_g}) = 0$$

$$b_{n_2}' = - \frac{V^2}{gc} \cdot z_{\dot{\alpha}_g}$$

$$b_{n_1}' = \frac{V^2}{gc} (z_{\dot{\alpha}_g} \cdot m_q - m_{\dot{\alpha}_g} \cdot z_q + \frac{V}{c} \cdot m_{\dot{\alpha}_g})$$

$$b_{n_o}' = - \frac{V^2}{g\bar{c}} \left(z_\alpha \, m_{\dot{\alpha}_g} - m_\alpha \, z_{\dot{\alpha}_g} \right)$$

In a similar way, the resulting transfer function relating the angular acceleration $\frac{\dot{q}\bar{c}}{V}$ and the gust angle of attack is obtained:

$$H_{II}(\omega) = (H_{\dot{q}\alpha_g})_r \; (P) = H_3(P) + H_o(P) \; . \; H_4(P)$$

The transfer functions $H_3(P)$ and $H_4(P)$ are:

$$H_3(P) = P \; . \; \frac{b_{q_1} \, P + b_{q_o}}{P^2 + a_1 \, P + a_o}$$

$$H_4(P) = P \; . \; \frac{b_{q_1}' \, P + b_{q_o}'}{P^2 + a_1 \, P + a_o}$$

where:

$$a_1 = - \frac{V}{\bar{c}} \left(z_\alpha + m_q \right)$$

$$a_o = \frac{V}{\bar{c}} \; . \; \left(z_\alpha \, m_q - m_\alpha \, z_q \right)$$

$$b_{q_1} = \frac{V}{\bar{c}} \; . \; m_{\alpha_g}$$

$$b_{q_o} = - \frac{V}{\bar{c}} \; . \; \left(z_\alpha \, m_{\alpha_g} - m_\alpha \, z_{\alpha_g} \right) = 0$$

$$b_{q_1}' = \frac{V}{c} m_{\dot{\alpha}_g}$$

$$b_{q_o}' = - \frac{V}{c} (z_\alpha m_{\dot{\alpha}_g} - m_\alpha z_{\dot{\alpha}_g})$$

Replacing the complex variable P in the transfer function H(P) by the imaginary variable jω finally yields the transfer functions H(ω).

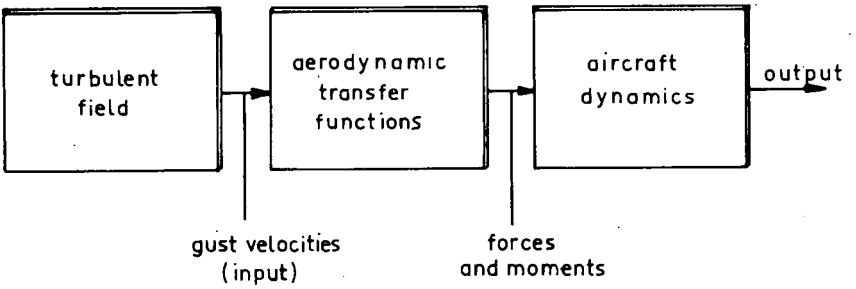

Fig. 1. The calculation of aircraft response to atmospheric turbulence.

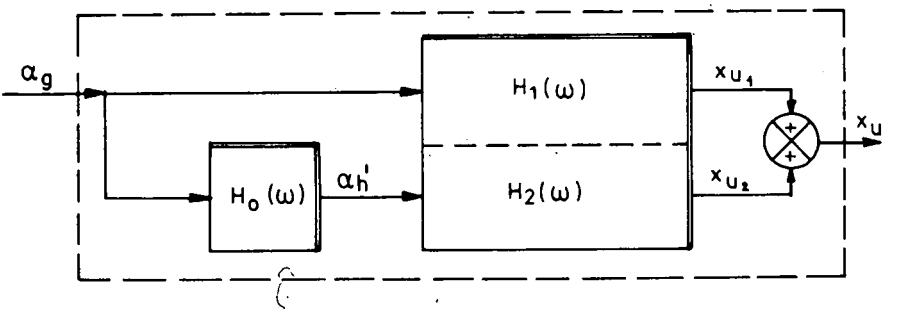

Fig. 2. Block-diagram of the aircraft perturbed by the input signals α_g and α_h'.

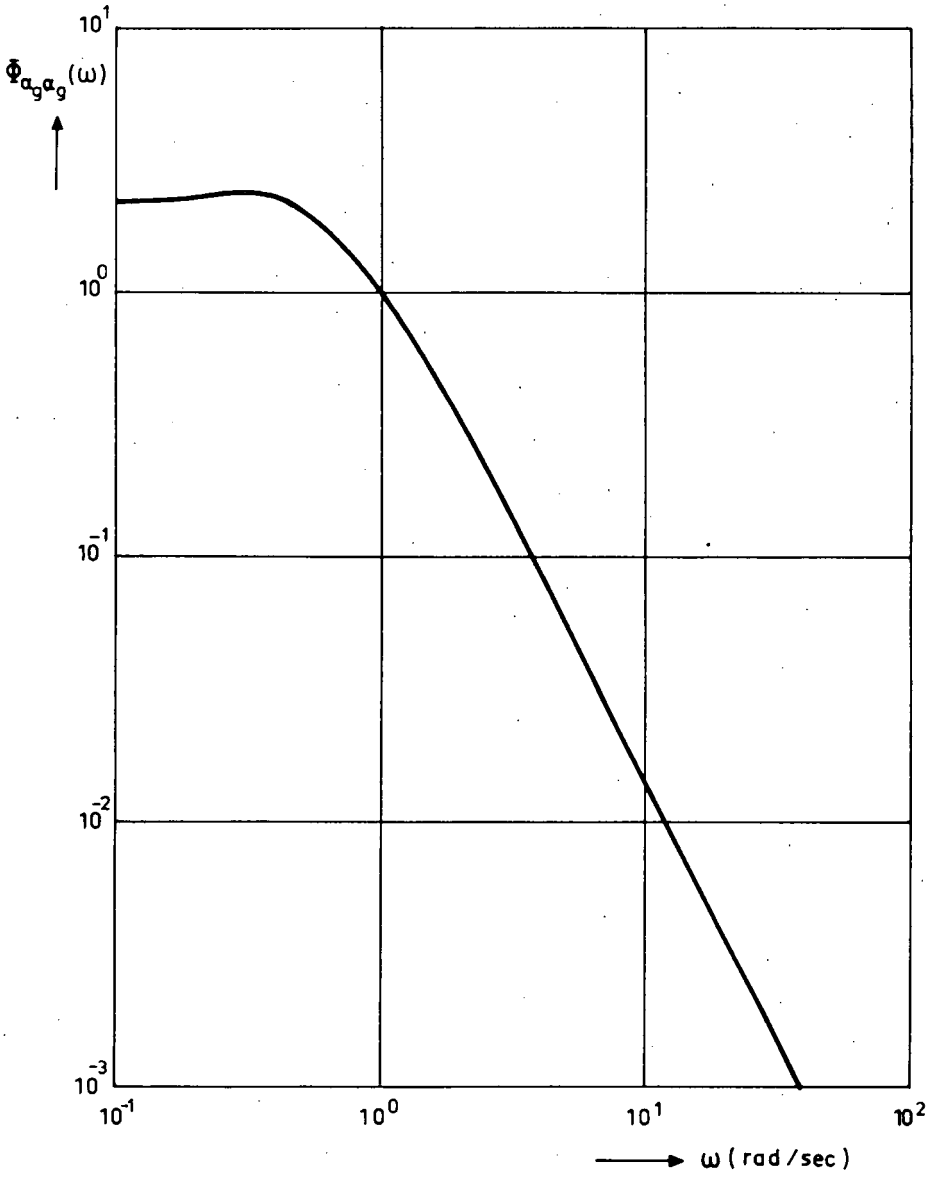

Fig. 3. Power spectral density of α_g according to Dryden.
σ_{α_g} = 1 rad, L_g = 150 m.

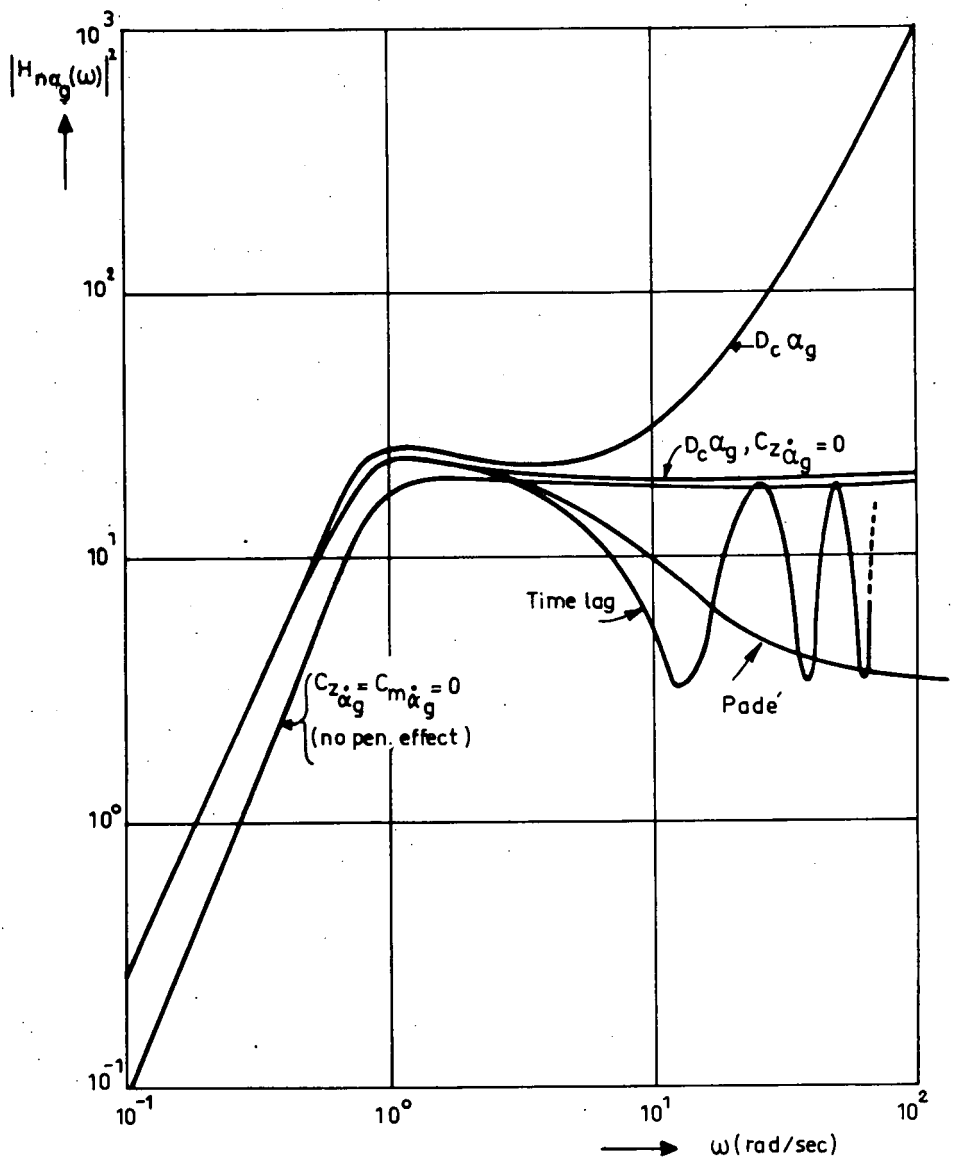

Fig. 4. Modulus squared of the transfer function $H_{n\alpha_g}(\omega)$ (constant speed).

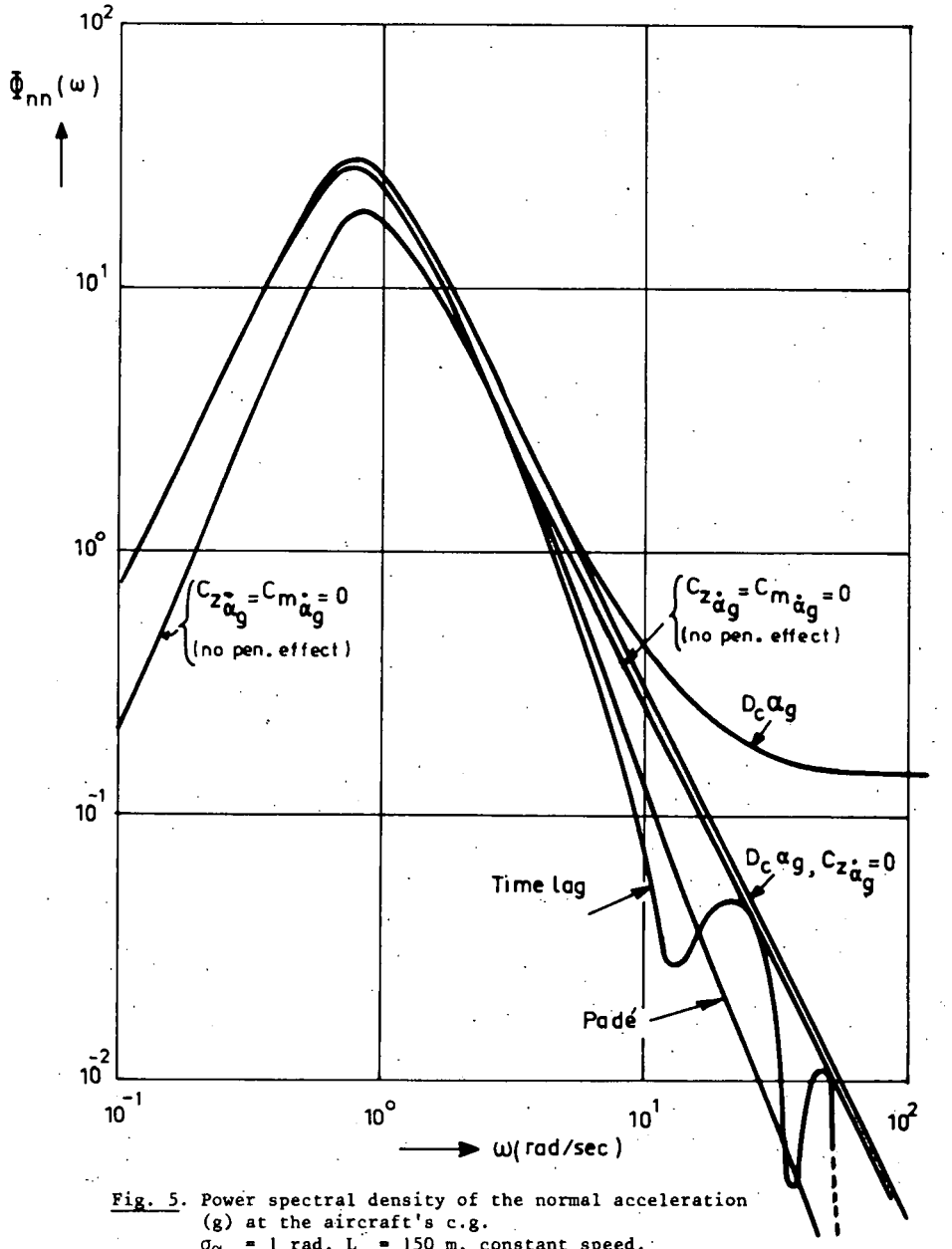

Fig. 5. Power spectral density of the normal acceleration (g) at the aircraft's c.g.
σ_{α_g} = 1 rad, L_g = 150 m, constant speed.

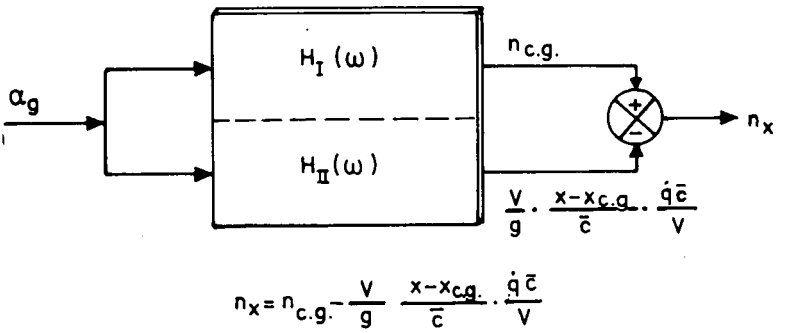

Fig. 6. Block-diagram for the calculation of the normal acceleration at some distance from the aircraft's c.g.

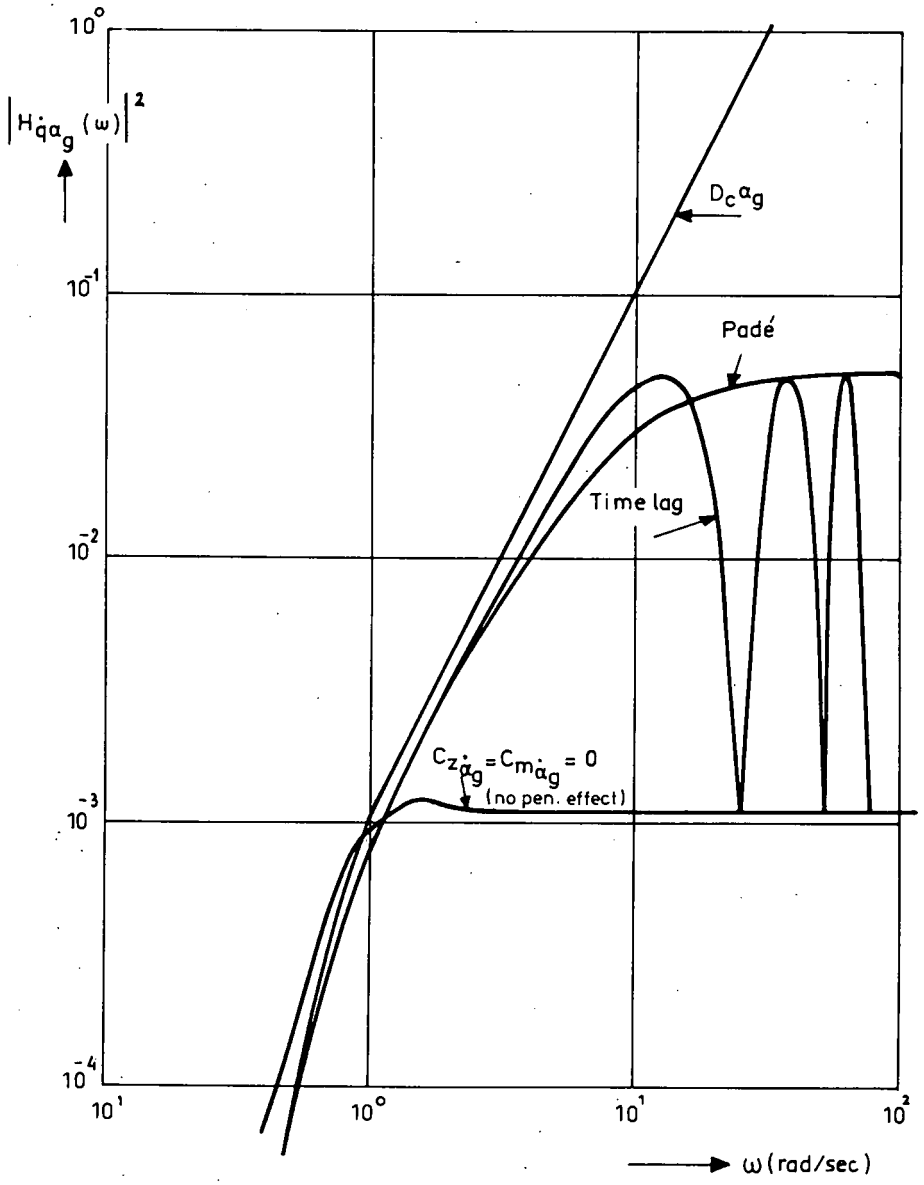

Fig. 7. Modulus squared of the transfer function $H_{\dot{q}\alpha_g}(\omega)$ (constant speed).

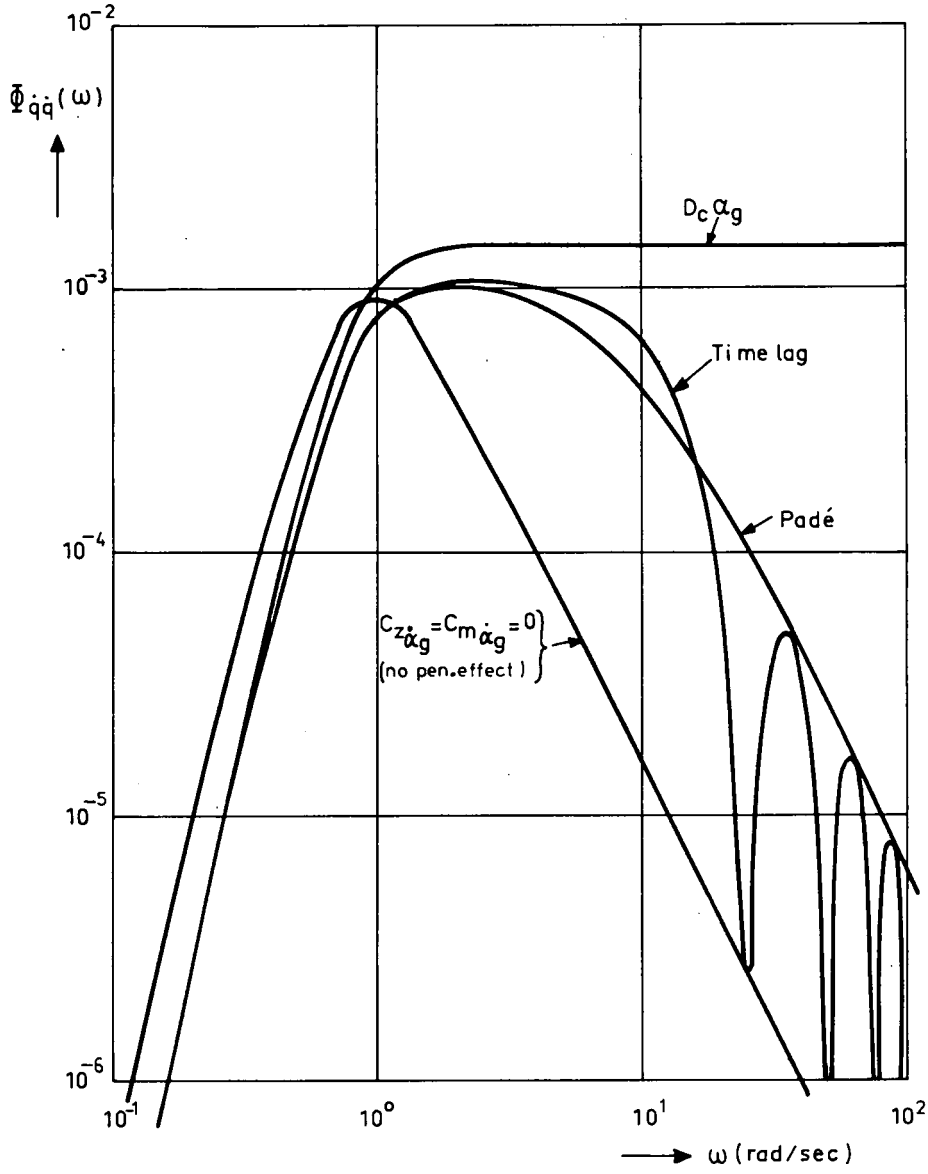

Fig. 8. Power spectral density of $\frac{\dot{q}\bar{c}}{V}$.
σ_{α_g} = 1 rad, L_g = 150 m, constant speed.

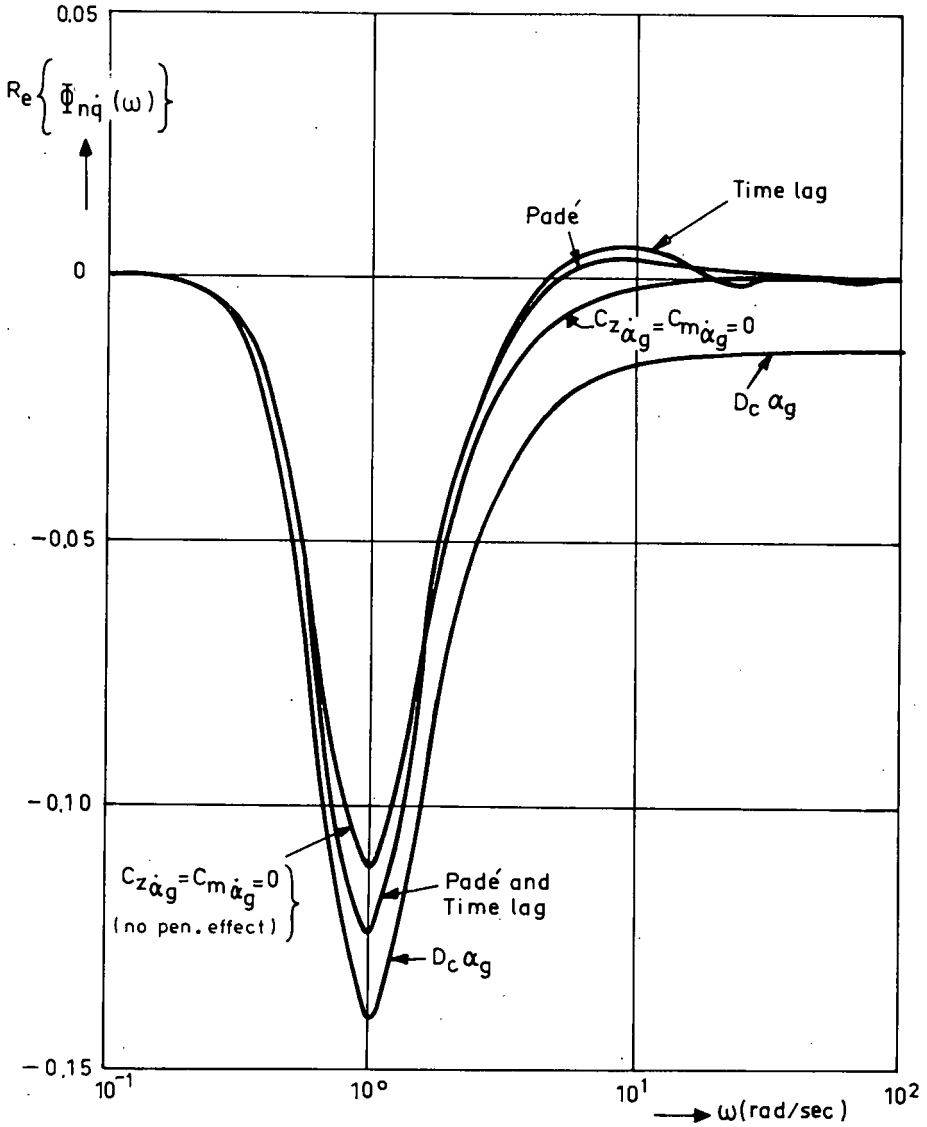

Fig. 9. Real part of the cross-power spectral density of n and $\frac{\dot{q}\bar{c}}{V}$.
σ_{α_g} = 1 rad, L_g = 150 m, constant speed.

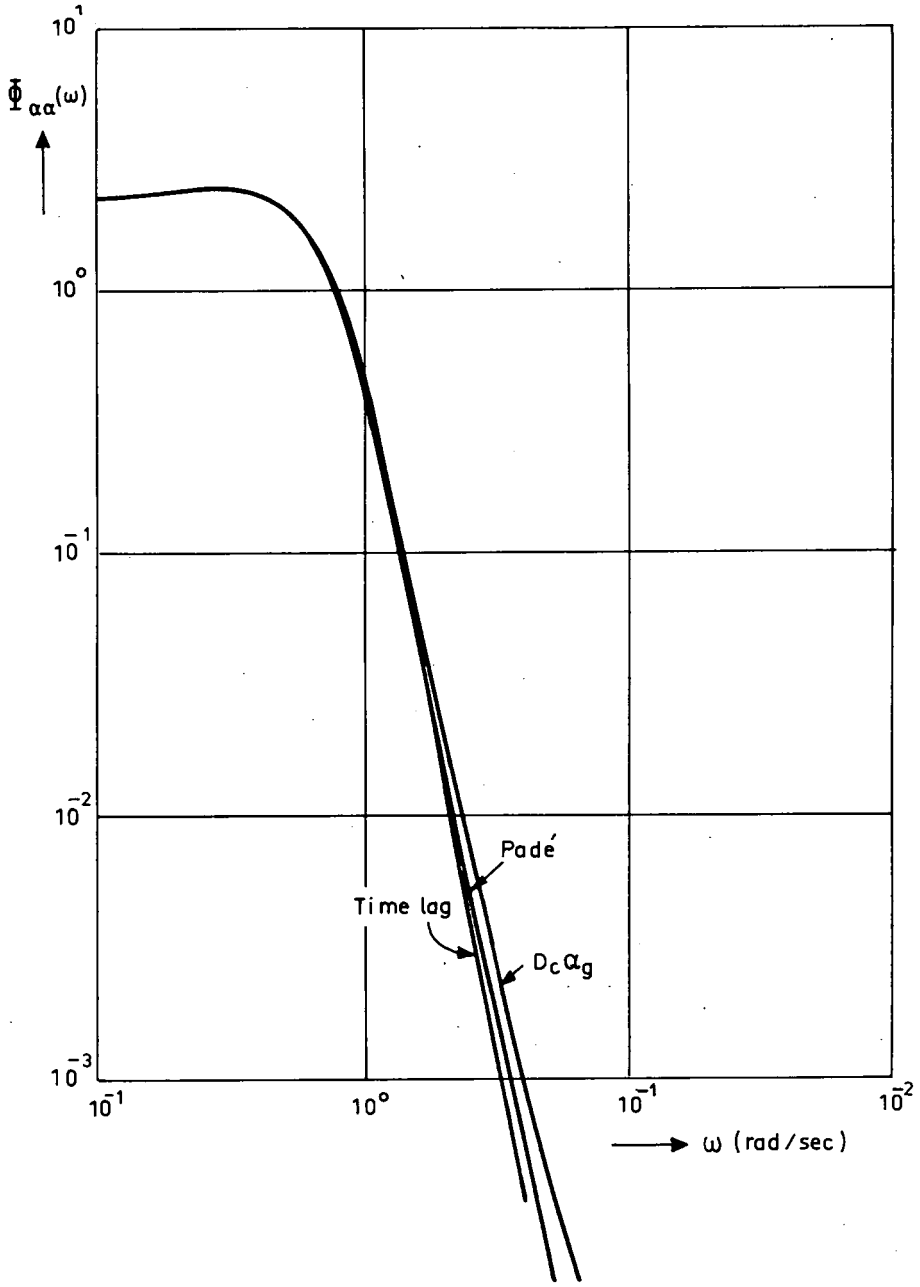

Fig. 10. Power spectral density of the angle of attack α.
σ_{α_g} = 1 rad, L_g = 150 m, constant speed.

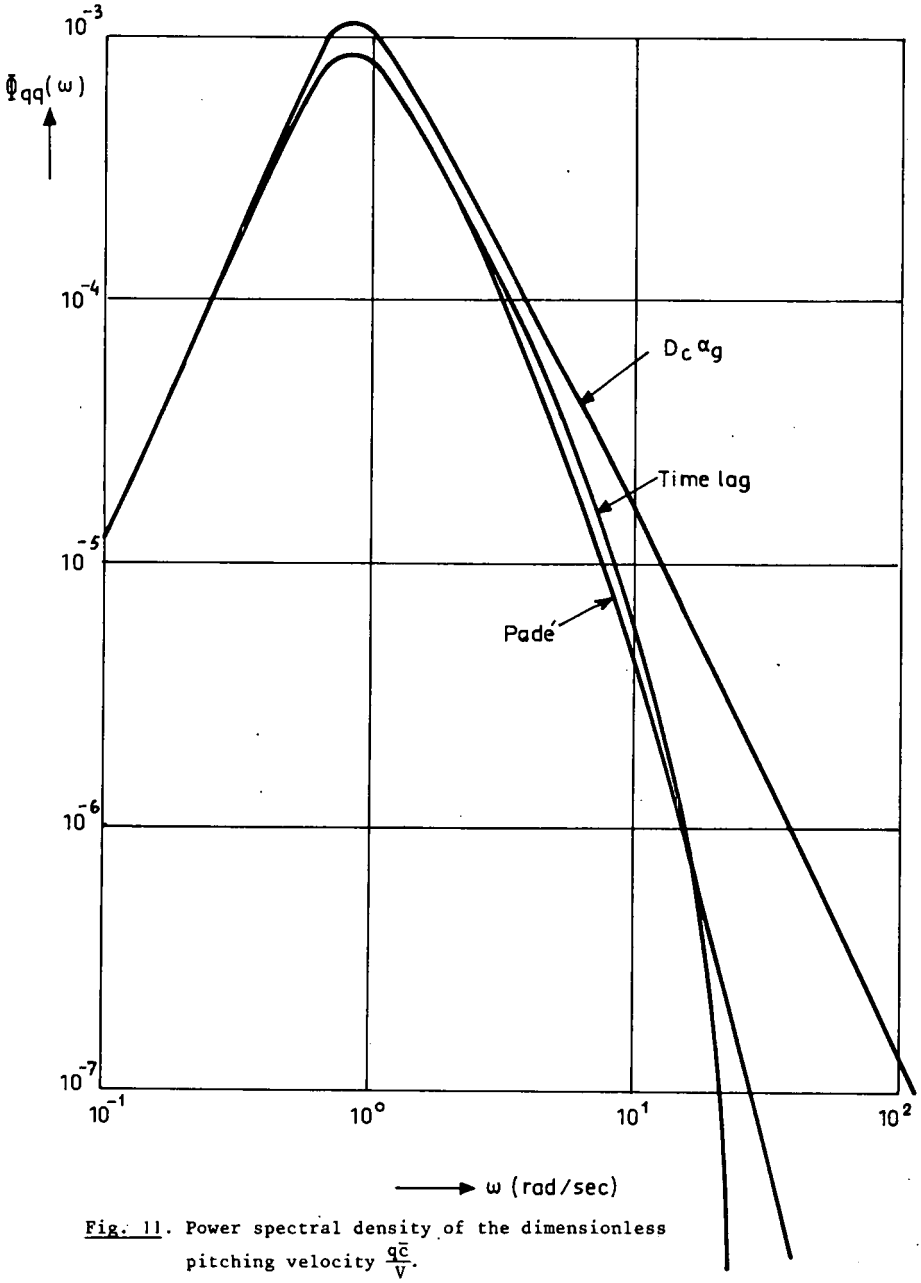

Fig. 11. Power spectral density of the dimensionless pitching velocity $\frac{q\bar{c}}{V}$.
σ_{α_g} = 1 rad, L_g = 150 m, constant speed.

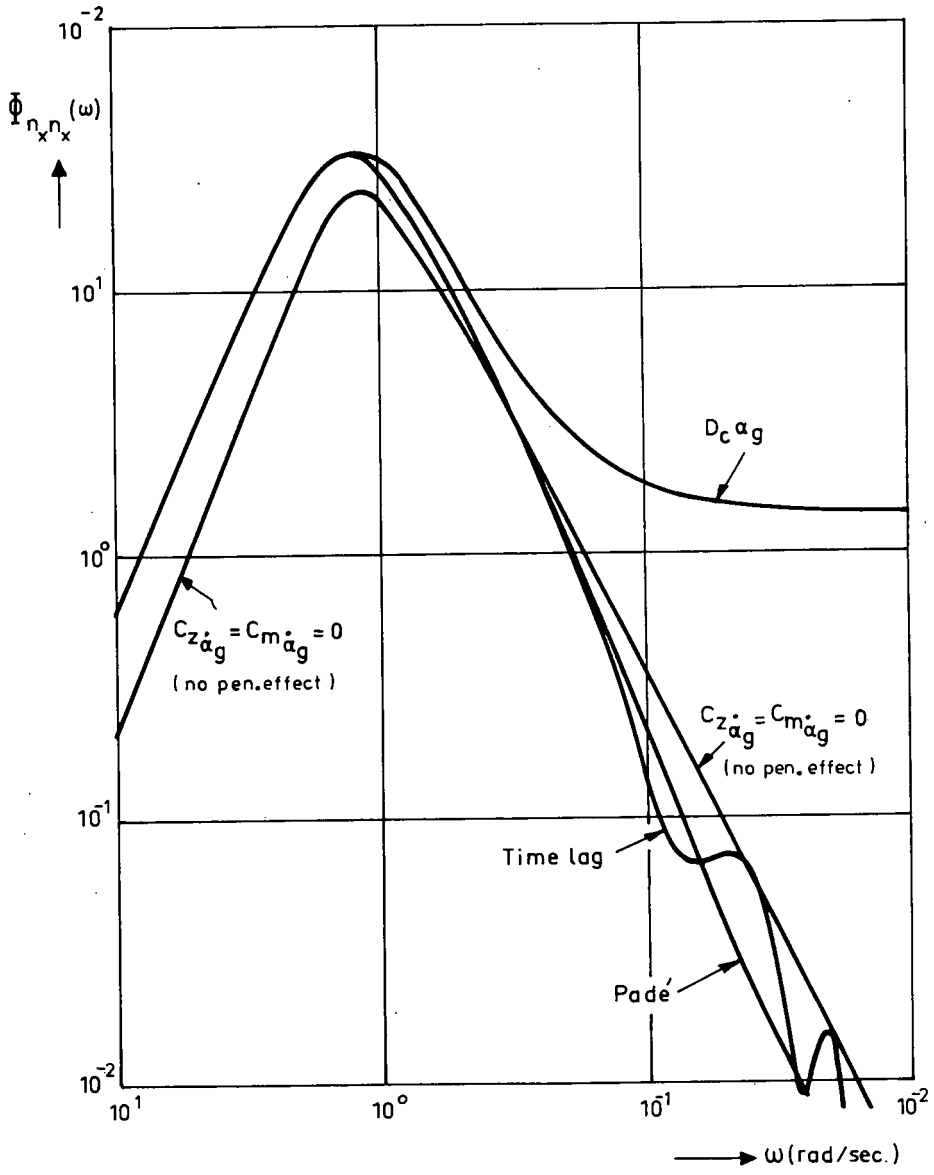

Fig. 12. Power spectral density of the normal acceleration (g) at the horizontal tail location $\left(\frac{x - x_{c.g.}}{\bar{c}} = 3{,}0\right)$.
σ_{α_g} = 1 rad, L_g = 150 m, constant speed.

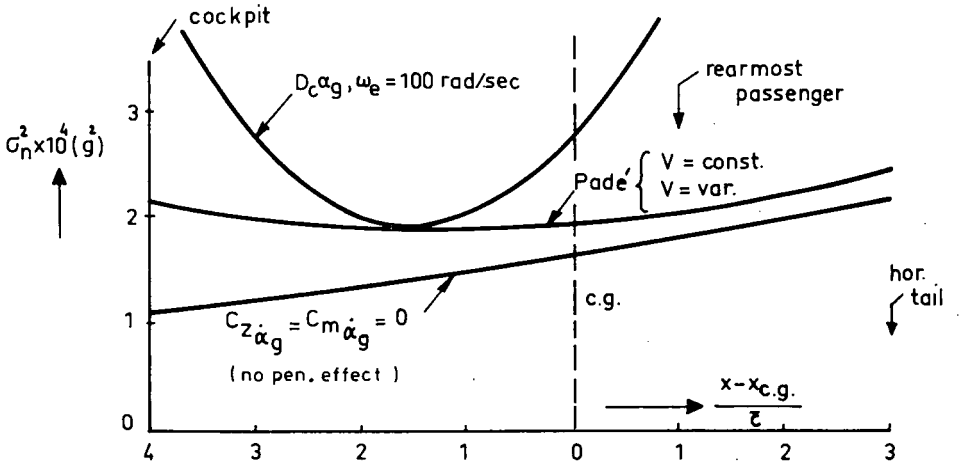

Fig. 13. Calculated variance of the normal acceleration as a function of the location along the X-axis of the example aircraft. σ_{w_g} = 0,282 m/sec, L_g = 150 m.

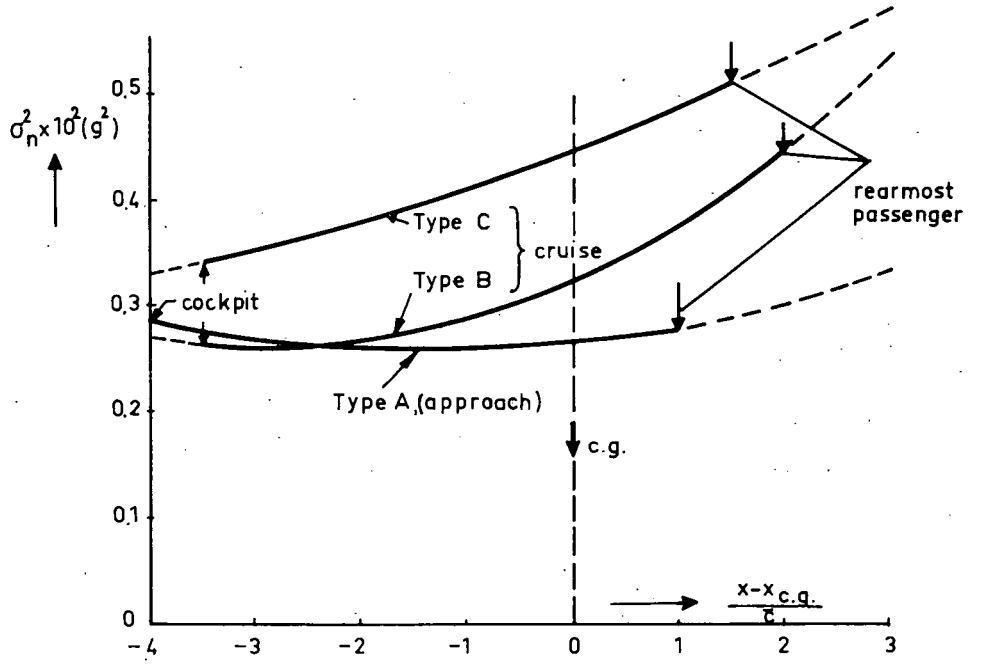

Fig. 14. Calculated variance of the normal acceleration as a function of the location along the X-axis of three different aircraft types (Padé approx.). σ_{w_g} = 1 m/sec; type A: L_g = 150 m, types B and C: L_g = 300 m.